Biochimica et Biophysica Acta 1838 (2014) 1344–1361

Contents lists available at ScienceDirect

Biochimica et Biophysica Acta

journal homepage: www.elsevier.com/locate/bbamem

Human heat shock protein 70 (Hsp70) as a peripheral membrane protein

Ajay K. Mahalka [a], Thomas Kirkegaard [b,c], Laura T.I. Jukola [a], Marja Jäättelä [b], Paavo K.J. Kinnunen [a,*]

[a] Helsinki Biophysics and Biomembrane Group, Department of Biomedical Engineering and Computational Science, Aalto University, Espoo, Finland
[b] Cell Death and Metabolism, Danish Cancer Society Research Center, Copenhagen, Denmark
[c] Orphazyme ApS, Copenhagen, Denmark

ARTICLE INFO

Article history:
Received 1 October 2013
Received in revised form 13 January 2014
Accepted 17 January 2014
Available online 28 January 2014

Keywords:
Hsp70
Liposomes
Tryptophan
Fluorescence
Extended lipid conformation
Langmuir-films

ABSTRACT

While a significant fraction of heat shock protein 70 (Hsp70) is membrane associated in lysosomes, mitochondria, and the outer surface of cancer cells, the mechanisms of interaction have remained elusive, with no conclusive demonstration of a protein receptor. Hsp70 contains two Trps, W90 and W580, in its N-terminal nucleotide binding domain (NBD), and the C-terminal substrate binding domain (SBD), respectively. Our fluorescence spectroscopy study using Hsp70 and its W90F and W580F mutants, and Hsp70-ΔSBD and Hsp70-ΔNBD constructs, revealed that binding to liposomes depends on their lipid composition and involves both NBD and SBD. Association of Hsp70 with phosphatidylcholine (PC) liposomes is weak, with insertion of its Trps into the bilayer hydrocarbon region. In the presence of cardiolipin (CL), bis-monoacylglycero phosphate (BMP), or phosphatidylserine (PS) Hsp70 attaches to membranes peripherally, without penetration. Our data suggest that the organelle distribution of Hsp70 is determined by their specific lipid compositions, with Hsp70 associating with the above lipids in mitochondria, lysosomes, and the surface of cancer cells, respectively. NBD and SBD attach to lipids by extended phospholipid anchorage, with specific acidic phospholipids associating with Hsp70 in the extended conformation with acyl chains inserting into hydrophobic crevices within Hsp70, and other chains remaining in the bilayer. This anchorage is expected to cause a stringent orientation of Hsp70 on the surface. Our data further suggest that acidic phospholipids induce a transition of SBD into the molten globule state, which may be essential to allow SBD–substrate interaction also within the hydrophobic bilayer interior acyl chain region.

1. Introduction

Heat shock protein 70 (Hsp70) constitutes a highly conserved family of protein chaperones, which under physiological conditions regulate protein homeostasis and promote cell survival [1]. Some Hsps are constitutively expressed, whereas others are strictly stress-inducible [2]. The major stress-induced human Hsp70 (also referred to as Hsp72) is expressed when the cell is exposed to stress such as heat shock or UV radiation. *Escherichia coli* Hsp70 chaperone is DnaK, which is regulated by two protein modulators, DnaJ and GrpE [3]. *Saccharomyces cerevisiae* has several Hsp family members, the most studied of these being the cytosolic Ssa1p [3]. Eight different and unique Hsp70 have been reported to be present in eukaryote cells, distributed in different subcellular compartments, including cytosol, nucleus, endoplasmic reticulum, and mitochondria [2]. The main function of these ubiquitous chaperones is to bind to denatured proteins and to assist in their refolding, in order to prevent their aggregation, and to guide them to their native conformations, in a manner requiring ATP [4], thus preventing cellular damage and apoptosis induced by unfolded aggregated proteins [5]. Hsp70s consist of two domains: NBD (residues 1–386) and the C-terminal substrate binding domain (SBD, residues 386–640, [6], Fig. 1, panel A). Three distinct conformations: nucleotide free, ADP-dependent, and ATP-dependent, have been demonstrated for *E. coli* DnaK [7]. The

Abbreviations: AcrA, acrylamide; aSM, acid sphingomyelinase; a.u., arbitrary unit; BMP, bis(monoacylglycero)phosphate; Br_2PC, brominated phosphatidylcholine; 6,7Br_2-PC, 1-palmitoyl-2-(6,7-dibromo)stearoyl-*sn*-glycero-3-phosphocholine; 9,10Br_2-PC, 1-palmitoyl-2-(9,10-dibromo)stearoyl-*sn*-glycero-3-phosphocholine; 11,12Br_2-PC, 1-palmitoyl-2-(11,12-dibromo)stearoyl-*sn*-glycero-3-phosphocholine; Br_4BMP, bis[mono(9,10)-dibromostearoyl] glycerophosphate; 9,10Br_2-PS, 1-palmitoyl-2-(9,10-dibromo)stearoyl-*sn*-glycero-3-phospho-L-serine; Br_8CL, tetra(9,10-dibromo stearoyl)cardiolipin; Br_2PS, brominated phosphatidylserine; CD, circular dichroism; Chol, cholesterol; CL, cardiolipin; DnaK, *E. coli* heat shock protein 70; DTT, dithiothreitol; EDTA, ethylenediamine-N,N,N′,N′-tetraacetic acid; F, fluorescence intensity; F_0, initial fluorescence intensity; FA, fatty acid; Grp78, endoplasmic reticulum heat shock protein 70; HD, Huntington disease; HDP, host defense peptides; Hepes, 4-(2-Hydroxyethyl)-1-piperazineethanesulfonic acid; Hsc70, constitutively expressed heat shock protein 70; Hsp70, Heat shock protein of ≈70kDa; Hsp70-ΔNBD, recombinant Hsp70 lacking the nucleotide binding domain; Hsp70-ΔSBD, recombinant Hsp70 lacking the substrate binding domain; Hsp70-W90F, recombinant Hsp70 with substitution W90F; Hsp70-W580F, recombinant Hsp70 with substitution W580F; KCL, potassium chloride; K_{sv}, Stern–Volmer quenching constants; L/P, lipid/protein molar ratio; LUV, large unilamellar vesicles; MES, 2-(*N*-morpholino)ethanesulfonic acid; NBD, nucleotide binding domain; NPD, Niemann–Pick disease; PEG, polyethylene glycol; POPC, 1-palmitoyl-2-oleoyl-*sn*-glycero-3-phosphocholine; POPS, 1-palmitoyl-2-oleoyl-*sn*-glycero-3-phospho-L-serine; PS, phosphatidylserine; RFI, relative fluorescence intensity; Spm, sphingomyelin; SBD, substrate binding domain; Ssa1p, *S. cerevisiae* heat shock protein 70; tOCL, 1,1′,2,2′-tetraoleoyl cardiolipin; wtHsp70, wild type Hsp70; π, surface pressure; π_0, initial surface pressure; $\Delta\pi$, increment in surface pressure; π_c, critical packing pressure; λ, wavelength; $\Delta\lambda$, spectral center of mass

* Corresponding author at: Helsinki Biophysics & Biomembrane Group, Department of Biomedical Engineering and Computational Science, P.O. Box 12200 (Rakentajanaukio 3), FIN-00076, Aalto, Finland. Tel.: +358 50 540 4600; fax: +358 9 470 23182.
E-mail address: paavo.kinnunen@aalto.fi (P.K.J. Kinnunen).

0005-2736/$ – see front matter © 2014 Elsevier B.V. All rights reserved.
http://dx.doi.org/10.1016/j.bbamem.2014.01.022

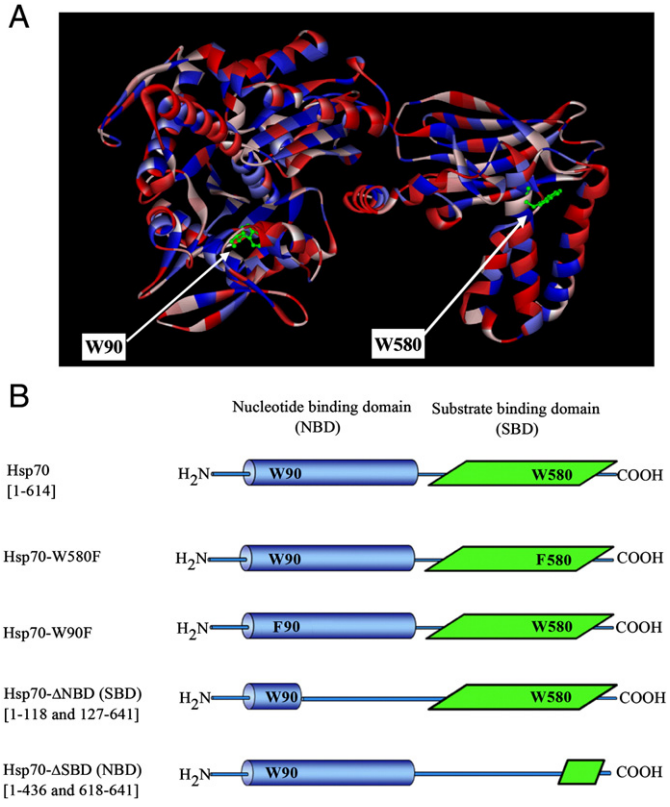

Fig. 1. Panel A: Tentative 3D ribbon structure of Hsp70 based on the crystal structures of bovine Hsc70 (PDB ID: 1YUW) and SBD of Hsp70 (PDB ID: 2P32), homology modeled by the Discovery studio. Surface coloring illustrates hydrophobicity (blue) and hydrophilicity (red). W90 and W580 are shown as ball and stick models (green). Panel B: Hsp70 constructs used in the present study.

conformations of NBD and SBD have been shown to be coupled for Hsp70 [8], DnaK [7], and Grp78 [9]. The presence of ATP accelerates the binding and release of polypeptides, but it still remains unclear whether it is the binding or hydrolysis of ATP that causes the release of peptides from SBD [8]. Formation of dimers and higher-order oligomers of Hsp70 has been suggested, with the monomeric protein representing the functionally active chaperone [10,11].

Hsp70 is additionally involved in the control of cell signaling for growth, differentiation, and apoptosis [12,13] and its overexpression is required for the growth and survival of human tumors [12–15], with elevated expression of Hsp70 correlating with poor prognosis in human breast cancer and endometrial tumors [16,17]. Hsp70 is highly expressed in the cytosol, outer surface of the plasma membrane and the membranes of the endo-lysosomal compartment in primary tumors of different origins, whereas its expression in unstressed normal cells is low and restricted to the cytosol [18–22].

Hsp70 may also provide a recognition structure for natural killer cells [23]. Multiple reports have demonstrated the association of Hsp70 family members with biomembranes in normal and tumor cells, and tumor-derived cell lines [21,23–26]. Bovine Hsc70 binds to cell surface sulfogalactolipids through its N-terminal nucleotide binding domain (NBD, [27]). Electron microscopy shows Hsp70 on the cell surface, in clathrin coated pits, and within endosome/lysosome-related vesicles [28]. There is also evidence that Hsp70 is associated with the so-called detergent resistant microdomains in the plasma membrane [29].

Direct interaction of Hsp70 with bis-monoacylglycero phosphate (BMP), an acidic phospholipid enriched in late endosomes and lysosomes [30] appears to be required for the activation of lysosomal acid sphingomyelinase (aSM), whose activity is essential for the downstream cytoprotective effect of lysosomal Hsp70. Our previous studies revealed that NBD contains a specific and pH-dependent binding site for BMP. Trp90 of NBD is required for this interaction and its mutation to Phe results in an Hsp70 with compromised BMP-binding, rendering Hsp70 unable to prevent lysosomal membrane permeabilization [30]. This interaction can also be blocked by an antibody against BMP [30].

Despite the accumulating information on the membrane association of Hsp70 and its potential significance to the functions of Hsp70, lipid–Hsp70 interactions have not been assessed in detail. Accordingly, the exact molecular mechanisms and the mode of attachment of Hsp70 to membrane bilayers remain to be elucidated. Intriguingly, Hsp70 has been demonstrated to contain two fatty acid binding sites. Membrane association of Hsp70 and its lipid-interactions demonstrated so far already suggest that Hsp70 could be a peripheral membrane protein. In this study, we exploited the intrinsic Trp fluorescence of human Hsp70 to evaluate possible lipid specificity in the membrane binding of Hsp70. Two mutants, Hsp70-W90F and Hsp70-W580F as well as NBD and SBD constructs Hsp70-ΔSBD and Hsp70-ΔNBD were additionally compared with wtHsp70 for their interactions with 1-palmitoyl-2-oleoyl-*sn*-glycero-3-phosphocholine (POPC), as well as cardiolipin (CL), BMP, and 1-palmitoyl-2-oleoyl-*sn*-glycero-3-phospho-L-serine (POPS) containing PC liposomes, complementing our previous studies on BMP [30], and those by Arispe et al. [31] on PS.

The aim of the present study was to explore in more detail the interactions of Hsp70 and NBD and SBD with different lipids, providing at this stage a qualitative understanding of the interactions and how they influence the orientation and conformation of Hsp70 in membranes. Our present results demonstrate a complex array of interactions of Hsp70 with phospholipid membranes. These interactions are highly sensitive to the membrane lipid composition, with Hsp70 selectively binding to membranes containing negatively charged phospholipids such as CL, BMP, and PS. Accordingly, the distribution of Hsp70 in lysosomes, mitochondria, and on the outer surface of cancer cells, respectively, could reflect the enrichment of these lipids in the above organelles and their interactions with Hsp70. Using single Trp Hsp70 mutants W90F and W580F we showed that both NBD and SBD contribute to the attachment of Hsp70 to lipid surfaces. In NBD the phospholipid binding site involves W90, which is also involved in the cationic site responsible for the binding of ATP [32]. Our data derived from Langmuir balance and Trp fluorescence spectroscopy experiments using collisional quenching by brominated phospholipids (6,7-Br_2PC, Br_2PS, Br_4BMP, and Br_8CL), and acrylamide as well as wtHsp70, its W90F and W580F mutants, and the NBD and SBD constructs allow us to conclude that

(i) Hsp70 binds to CL, BMP, and PS containing membrane surfaces peripherally, most likely by extended phospholipid anchorage [33,34].
(ii) Both NBD and SBD appear to interact with lipids.
(iii) Our data further suggest that under these conditions SBD is likely to adopt the molten globule conformation.

2. Experimental procedures

2.1. Materials

1-Palmitoyl-2-oleoyl-*sn*-glycero-3-phosphocholine (POPC), 1-palmitoyl-2-(6,7-dibromo)stearoyl-*sn*-glycero-3-phosphocholine (6,7Br_2-PC), 1-palmitoyl-2-(9,10-dibromo)stearoyl-*sn*-glycero-3-phosphocholine (9,10Br_2-PC), 1-palmitoyl-2-(11,12-dibromo)stearoyl-*sn*-glycero-3-phosphocholine (11,12Br_2-PC), 1-palmitoyl-2-oleoyl-*sn*-glycero-3-phospho-L-serine (POPS), 1,1′,2,2′-tetraoleoyl cardiolipin (toCL), bis-monoacylglycero phosphate (BMP), cholesterol, N-acyl-phosphatidylethanolamine, and sphingomyelin were from Avanti Polar-Lipids Inc. (Alabaster, AL, USA). PEG 400 was from ABCR GmbH & Co.KG (Karlsruhe, Germany). Lipids were dissolved in chloroform and their concentrations were determined gravimetrically using a high precision electrobalance (Cahn, Cerritos, CA) as described

previously [35]. Acrylamide (AcrA, 99% purity) was from Eastman-Kodak (Rochester, NY, US). All other chemicals were of analytical grade from standard sources.

2.2. Expression and purification of Hsp70

wtHsp70, Hsp70-W580F, Hsp70-W580F, Hsp70-ΔNBD, and Hsp70-ΔSBD constructs (Fig. 1, panel B) were generated using the pET-16b vector system and Ni^{2+}-affinity-purification system (Novagen, Merck KGaA, Darmstadt, Germany). The recombinant Hsp70 constructs containing His^6-tag were separated using a Ni^{2+}-column, with the bound protein eluted with 0.5 mM imidazole at pH 7.4, subsequently medium exchanged for Dulbecco's phosphate buffered saline (D-PBS) using chromatography over a PD10 column (Amersham). The factor Xa recognition site located between the His^6-tag and the Hsp70 domains was then cleaved by factor Xa and the His^6-tag and factor Xa removed by filtering through Amicon Ultra 50MWCA (Amersham). The purified Hsp70 constructs were stored at −20 °C in 25 mM Hepes, 0.1 mM EDTA, 10% glycerol, 50 mM KCL, 1 mM DTT, and pH 7.6. Charges of Hsp70 and its constructs at pH 7.4 and 6.0 were estimated with the web-based calculator (http://www.scripps.edu/~cdputnam/protcalc.html).

Importantly, our attempts to utilize His-tag containing proteins showed, that this addition has a significant influence on the lipid binding properties of Hsp70 (Mahalka et al., to be published), yielding constructs, which deviated drastically in their lipid binding properties from the wild-type protein. This behavior appears to result from the binding of His-tag to phospholipids.

2.3. Preparation of liposomes

Lipids were dissolved and mixed in chloroform to obtain the indicated compositions, where after this solvent was removed under a stream of nitrogen. The lipid residues were subsequently maintained under reduced pressure for at least 2 h and subsequently hydrated for 60 min at 60 °C in 20 mM Hepes, 0.1 mM EDTA to yield a lipid concentration of 2 mM. pH of the buffers was adjusted with HCl to pH 7.4 or 6.0 as indicated. In order to obtain large unilamellar vesicles (LUV), the hydrated lipid mixtures were extruded through 100 nm pore size polycarbonate membranes (Nucleapore Inc., Pleasanton, CA, USA) with a LiposoFast small-volume homogenizer (Avestin, Ottawa, Canada, [36]), yielding vesicles with mean diameters of 120–140 nm measured by dynamic light scattering.

2.4. Tryptophan fluorescence spectroscopy

All fluorescence measurements were conducted with a Perkin-Elmer LS50B spectrofluorometer. Hsp70 and buffer (20 mM Hepes, 0.1 mM EDTA, pH 7.4 or 6.0, total volume 2 ml) were mixed in a magnetically stirred PEG-treated [37] quartz cuvettes, with 10 mm optical path length in a holder thermostated at 37 °C with a circulating waterbath. Coating of the quartz glass cuvettes by PEG was used to minimize the binding of the Hsp70 to the cuvettes [37]. The initial concentration of Hsp70 in the cuvette was 0.43 μM in the indicated buffers. Trp emission was recorded between 308 and 450 nm with excitation and emission bandwidths of 10 nm and with excitation at 295 nm. When indicated liposomes were added in ten subsequent 20 nmol aliquots (in 10 μl) into the cuvette and spectra recorded after a 20 min stabilization period for each addition. From these data the emission peak positions, peak intensities, and spectral centers of mass were determined.

Brominated lipids were used to monitor possible contacts of the Trp residues of Hsp70 with the lipid acyl chains [38]. BMP, POPS, and tOCL were brominated as described by East and Lee [39] to yield bis[mono(9,10)-dibromostearoyl]glycerol-phosphate (Br_4BMP), 1-palmitoyl-2-(9,10-dibromo)-stearoyl-*sn*-glycero-3-phospho-L-serine (Br_2PS), and tetra(9,10-dibromostearoyl) cardiolipin (Br_8CL). Liposomes containing brominated phospholipids (6,7-Br_2PC, 9,10Br_2-, and 11,12Br_2PC, Br_2PS, Br_4BMP, or Br_8CL) were added into a solution of Hsp70 as above, and the ratios (F_0/F) of the Trp fluorescence peak intensities upon adding control liposomes and liposomes containing the indicated brominated lipids, respectively were calculated from the emission spectra. Differences in the quenching of Trp fluorescence by (6,7)-, (9,10)-, and (11,12)-Br_2-PC were used to estimate by the parallax method the apparent depth of penetration of Hsp70 Trps into the lipid bilayers [40].

In order to determine the exposure of Trps to the aqueous phase, AcrA, a water-soluble collisional quencher [41], was added as six subsequent micromolar aliquots. Spectra were recorded using excitation at 295 nm to minimize inner filter effect due to AcrA. All data have been subtracted for background and light scattering due to liposomes, normalized, and corrected for volume changes and the inner filter effect.

2.5. Binding of Hsp70 to lipid monolayers

Appropriate amounts of lipid stock solutions were mixed in chloroform to obtain the desired compositions. The indicated lipid mixtures were subsequently spread onto an air/buffer interface in magnetically stirred circular Teflon coated wells (diameter of 17.8 mm and a subphase volume of 1.2 ml) drilled in aluminum. Dynamic surface pressure (π) was monitored by the Wilhelmy technique using miniature cylindrical probes (Dyneprobe, Kibron Inc., Espoo, Finland) attached to the sensors of a four channel Langmuir tensiometer (DeltaPi-4, Kibron Inc.). Data were recorded using the embedded features of the instrument control software allowing for simultaneous monitoring of four reactions. After stabilization of the applied monolayers to a range of initial surface pressure values π_0 the indicated proteins were injected into the subphase (0.1 μM final concentration), where after the increment in π ($\Delta\pi$) due to their intercalation into the lipid film was recorded. These data are represented as $\Delta\pi$ vs π_0, yielding upon least-squares linear fitting straight lines with negative slopes. The *x*-axis intercepts represent critical lateral packing densities of lipids corresponding to surface pressure π_c, above which the protein no longer can intercalate into the monolayer [42]. All measurements were performed at ambient temperature of ~23 °C.

2.6. Circular dichroism (CD)

CD spectra were recorded with Olis RSF 1000F (On-line Instrument Systems Inc., Bogart, GA) CD spectrophotometer using a 0.1 mm optical path length quartz cuvette thermostated at 37 °C with a circulating waterbath. The instrument was calibrated with *d*-(+)-camphorsulfonic acid. Near and far UV-CD spectra were recorded from 260 to 198 nm, and 310 to 145 nm, respectively, at increment of 1 nm with 1 s integration time. To remove chloride and DTT aliquots of Hsp70 stock solution were dialyzed against MES buffer. The concentration of Hsp70 used in far and near UV-CD were 2 and 8.5 μM, respectively in a final volume of 2 ml of 20 mM MES, 0.1 mM EDTA at pH 6.0. All spectra have been corrected for circular differential scattering due to buffer and liposomes. The spectra shown represent the averages of four scans, and were analyzed with the computer program K2d2 [43].

3. Results

3.1. Lipid–protein interactions of Hsp70

We investigated the interactions of wtHsp70 with liposomes composed of POPC together with a range of different acidic phospholipids. To begin with, we first assessed the association of Hsp70 with the liquid expanded (fluid) state zwitterionic POPC, and then proceeded to compare this with its binding to POPC liposomes containing cardiolipin, BMP, and phosphatidylserine.

3.1.1. Binding of Hsp70 to phosphatidylcholine liposomes

Fluorescence spectroscopy of Trp provides a sensitive tool to obtain information on changes in protein conformation and interactions with *e.g.* lipids [44]. Human Hsp70 contains two Trps, W90 and W580, in its NBD and SBD, respectively (Fig. 1, panel B). Steady state Trp fluorescence emission depends on solvent polarity, and reflects in part the exposure of this residue to water [45]. Emission of Hsp70 in buffer was sensitive to pH with nearly identical spectral centers of mass observed at both pH 7.4 and 6.0, yet with approximately 30% higher overall emission evident at more acidic pH (Fig. 2). Augmented quantum yields at pH 6.0 were also seen for both Hsp70-W90F and Hsp70-W580F, thus suggesting that at pH 6.0 NBD and SBD both adopt conformations in which the two Trps become embedded in more hydrophobic environments.

We first explored by Trp fluorescence the binding of wtHsp70 to POPC liposomes. POPC LUV induced profound changes in the Trp fluorescence of Hsp70 (Fig. 3), with a large increase in the relative fluorescence intensity (RFI), together with a decrease (blue shift) in the wavelength of maximal emission (λ_{max}), thus indicating an increase in the hydrophobicity of the environments accommodating either W90 or W580, or both (Fig. 3, panels C and D). Together with the above shift in λ_{max} POPC LUV also caused a narrowing of the major peak at $\lambda_{max} \approx 340$ nm seen in the absence of liposomes (Fig. 3). The RFI *vs* L/P curve, for POPC was biphasic at pH 7.4 (Fig. 3, panel E), with an initial linear component followed by a second linear component at L/P >150 (*i.e.* corresponding to a higher surface dilution of Hsp70). Especially at higher L/P ratios the RFI values equilibrated slowly, requiring up to 15–20 min. The curves reveal no sign of saturation thus indicating a low affinity interaction, most likely arising from weak, non-specific hydrophobic partitioning of Hsp70 to the POPC bilayer. These changes suggest that compared to Hsp70 in buffer, binding of Hsp70 to POPC liposomes causes at least one of its Trp residues to become accommodated in a more hydrophobic environment. Complementary fluorescence experiments and spectral characteristics of W90 and W580 (Table 1, see below) suggest that the Trp primarily contacting the POPC bilayer acyl chain region is W90 of NBD, which consistently emits at slightly shorter value for λ_{max}. Compared to the spectra measured in the presence of POPC LUV at pH 7.4 the values for RFI recorded at pH 6.0 are somewhat lower and the initial linear component seen at pH 7.4 spans only a narrow L/P range (Fig. 3, panels E & F).

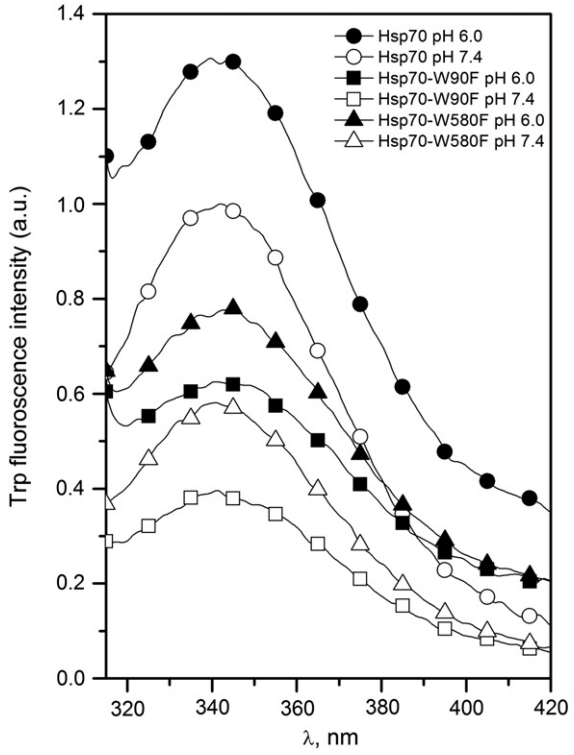

Fig. 2. Trp emission spectra in 20 mM Hepes, 0.1 mM EDTA for Hsp70 (○/●), Hsp70-W90F (W580, □/■), and Hsp70-W580F (W90, △/▲). Open symbols pH 7.4 and closed symbols pH 6.0. The concentrations of Hsp70 and the two mutants were 0.43 μM.

The above data complies with an intercalation of Hsp70 into POPC bilayers. In order to check for this possibility we investigated if phospholipids with brominated stearoyl chains, *i.e.* 6,7-, 9,10-, and 11,12Br_2-PC quench Trp fluorescence of Hsp70 bound to POPC liposomes. Bromine is a collisional quencher of Trp and in a bilayer in the absence of chain reversal the above phospholipid acyl chains should remain in the hydrophobic region of a bilayer. Trp fluorescence quenching by these three brominated PCs in POPC liposomes reveals contacts of the bromines with at least one of the Trp residues (Fig. 4, panel A). In a neutral bilayer and at pH 7.4 the Trp residue(s) in question seem(s) to reside in the vicinity of acyl chain carbon atoms 6,7 and 9,10. At pH 6 there is slightly less quenching, thus suggesting attenuated penetration of the Trp(s) into POPC bilayers (Fig. 4, panel B). This pH dependence could reflect an increase in the net charge of Hsp70 at pH 6.0, results in less penetration into the bilayer. Interestingly, quenching by 6,7-, and 9,10Br_2-PCs diminishes the blue shift in the spectral center of mass (Table SI). Since collisional quenching by Br should not alter the shape of the spectra, these data suggest that one of the Trp residues preferentially contacts the brominated acyl chains and becomes quenched, with less quenching of the fluorescence from Trp residing in a less hydrophobic environment and emitting at a longer λ_{max}. The latter Trps are likely to include the fraction of Hsp70 in solution (not attached to liposomes) and W580. Comparison of λ_{max} values for W90 and W580 (Table 1) suggests that the brominated PCs in POPC liposomes preferentially interact with NBD, quenching W90. From X-ray diffraction, the average distances of the bromines of 6,7-, 9,10-, and 11,12Br_2-PC, from the bilayer center are 10.8, 8.3, and 6.3 Å, respectively [38]. Parallax analysis [40] of our data suggests, that the distance of the Trp-residue (W90) quenched is approximately 11.5 Å from the bilayer center, thus indicating only a shallow insertion of W90 into the bilayer, in keeping with partitioning of Trp into the interfacial region of phospholipid bilayers [46].

In order to resolve the contributions of W90 and W580 to the above Trp fluorescence signals and the involvement of NBD and SBD in lipid interactions, we repeated the above experiments using Hsp70 mutants Hsp70-W90F and Hsp70-W580F. We previously showed that the W90F mutant fails to activate acid sphingomyelinase in cells, thus resulting in a lack of stabilization of lysosomal membranes when endocytosed. Interactions of Hsp70-W90F with liposomes containing BMP are impaired [30]. While F instead of W is generally considered to represent a minimally perturbing mutation, the activity of Hsp70 in cells is lost, revealing a crucial functional role of W90. The extent of perturbation of the overall conformation of Hsp70 and the lipid interactions of Hsp70 by the W90F mutation remain to elucidated. Yet, the results obtained from this construct allow us to decipher molecular level understanding of the phospholipid–Hsp70 interactions. Comparison of the spectra of Hsp70 and the above constructs (Fig. 2) reveals that the combined emission from W90 and W580 closely parallel the RFI of wtHsp70, thus suggesting that the overall conformations of the Trp-containing domains in these mutants are similar to those when present in the wtHsp70.

Similar to wtHsp70 a significant enhancement in Trp fluorescence is seen for the Hsp70-W580F as well as Hsp70-W90F in the presence of PC LUV (Fig. 5, panels A & B). Accordingly, the non-specific, low affinity interaction of Hsp70 with POPC liposomes seems to involve contributions from both NBD and SBD, most likely driven by hydrophobicity, and with intercalation of Trp-containing sequences into the lipid hydrocarbon region. 6,7-Br_2PC quenching data reveal contacts of both NBD and SBD Trps with the POPC bilayer region at both pH 7.4 and 6.0 (Fig. 6, panels A & B), with more pronounced quenching of W90. The above conclusion is supported by large fluorescence enhancement of Hsp70-W580F

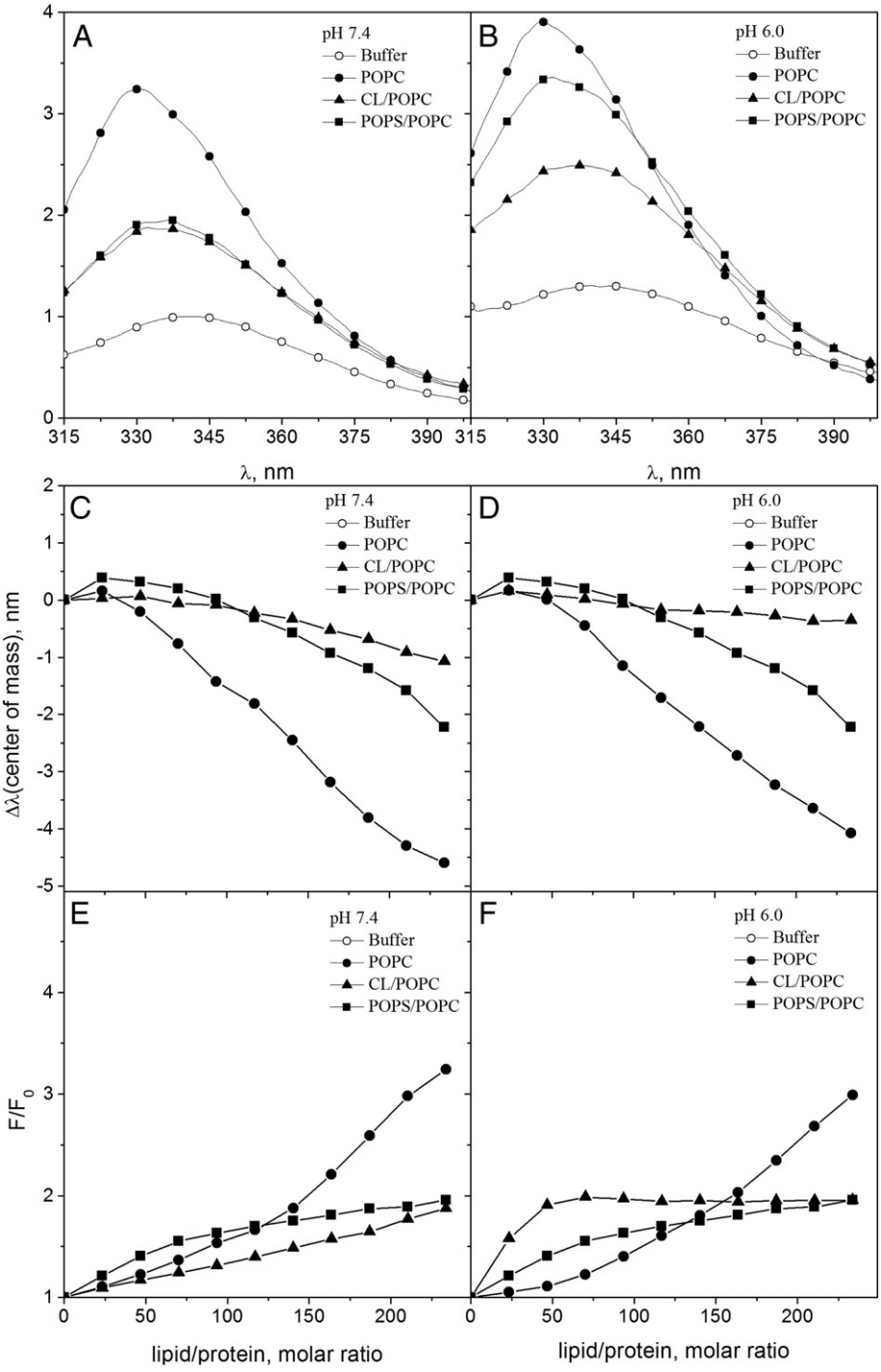

Fig. 3. Tryptophan fluorescence spectra for wtHsp70 (○) in buffer (20 mM Hepes, 0.1 mM EDTA) and in the same buffer in the presence of 95 μM (total lipid) LUV at pH 7.4 (panel A) and 6.0 (panel B). The effects of lipid binding on the decrement in the spectral center of mass ($\Delta\lambda$) for Hsp70 Trp fluorescence at pH 7.4 (panel C) and 6.0 (panel D) and the relative fluorescence intensity (F/F_0) at pH 7.4 (panel E) and 6.0 (panel F). LUV were composed of POPC (●), CL/POPC ($X_{CL} = 0.2$, ▲), and POPS/POPC ($X_{POPS} = 0.2$, ■). Initial protein concentration was 0.43 μM and the total concentration of lipids were increased in 10 μM increments up to 100 μM.

compared to Hsp70-W90F (Fig. 5, panels A & B) and diminished extent of quenching of Hsp70-W90F by AcrA compared to Hsp70-W580F (Fig. 8, panels A & B). Moreover, comparison of λ_{max} values also suggests that the brominated PCs in POPC liposomes preferentially interact with NBD, quenching W90 (Table 1).

In order to verify the intercalation of Hsp70 into POPC bilayers we assessed the efficiency of quenching of Trp emission by the water-soluble collisional quencher acrylamide [AcrA, 45]. In keeping with the immersion of Hsp70 Trps into the POPC bilayer at pH 7.4, their quenching by AcrA was attenuated in the presence of POPC LUV (Fig. 7, panel A), suggesting shielding of the Trps from contacts with the water soluble AcrA upon the POPC bilayer–Hsp70 interaction. At pH 6.0, however more efficient quenching by AcrA becomes evident, showing an increased exposure to AcrA (Fig. 7, panel B), in keeping with a more superficial location of Hsp70 on the POPC bilayer surface at pH 6.0, as concluded from Trp fluorescence and quenching by brominated PCs (Fig. 3, panel B, Fig. 4, panel B). These data aligns with a shielding from AcrA of W90 in Hsp70-W580F in the presence of PC

Table 1
Values for the spectral center of mass (Δλ) for Hsp70, Hsp70-W90F, Hsp70-W580F, Hsp70-ΔNBD, and Hsp70-ΔSBD in buffer and with the indicated LUV at L/P ≈ 234 and at pH 7.4 and 6.0.

		Hsp70	Hsp70-W90F (W580)	Hsp70-W580F (W90)	Hsp70-ΔNBD (SBD)	Hsp70-ΔSBD (NBD)
Buffer	pH 7.4	341.9	341.9	341.9	342.8	341.2
	pH 6.0	341.8	341.9	342	342.2	341.2
POPC	pH 7.4	337.3	339.4	337.7	338.3	339.2
	pH 6.0	337.7	337.4	338.5	338.2	339.2
CL/PC ($X_{CL} = 0.2$)	pH 7.4	341.0	343.2	342.8	343.0	342.2
	pH 6.0	340.8	342.4	343.0	343.2	342.2
BMP/PC ($X_{BMP} = 0.2$)	pH 6.0	341.5	341.9	342.5	342.9	341.2
PS/PC ($X_{PS} = 0.2$)	pH 7.4	339.6	341.6	340.5	341.3	340.2
	pH 6.0	339.5	339.3	340.3	340.2	339.2

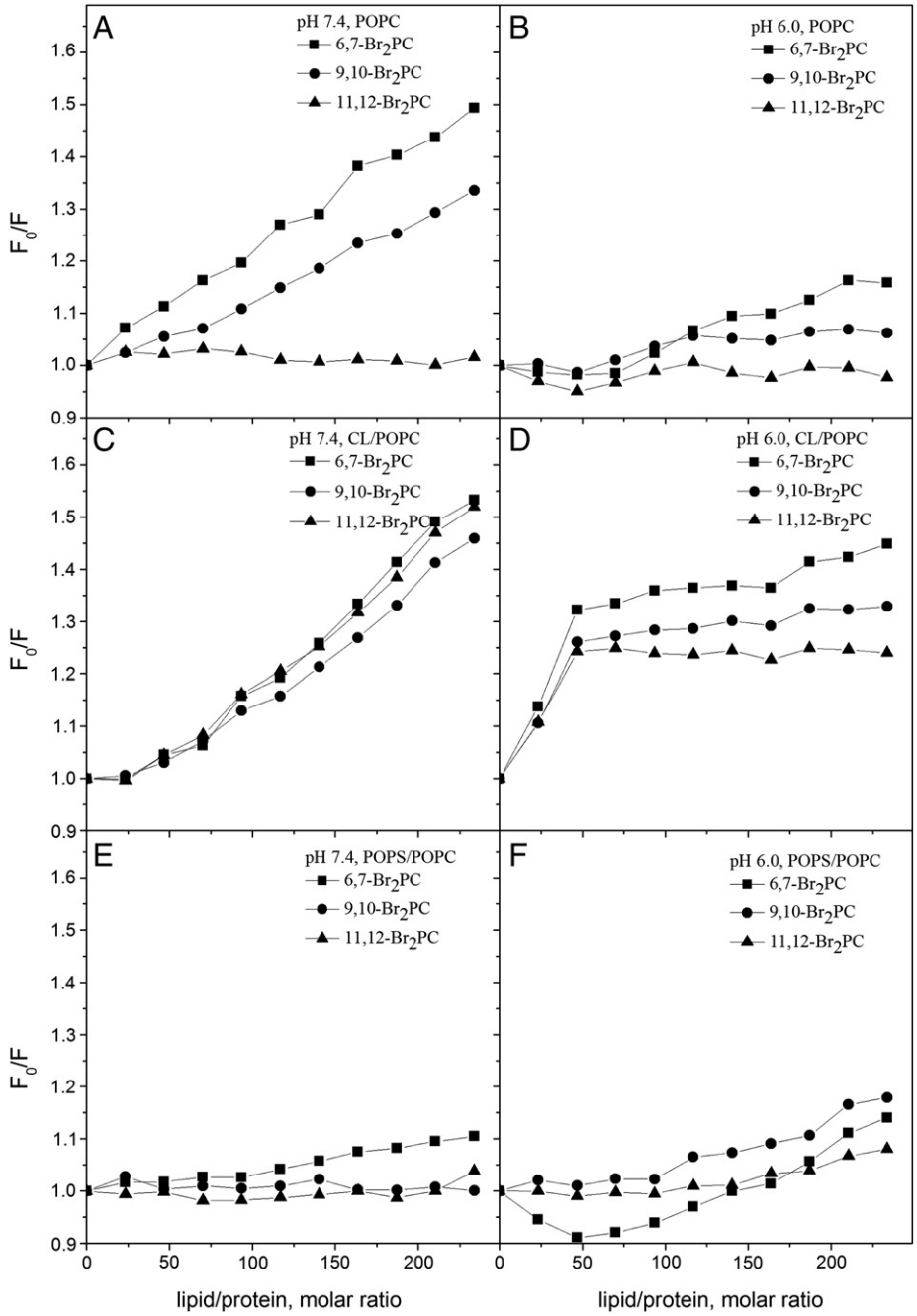

Fig. 4. Quenching of Hsp70 Trp fluorescence by 6,7-(■), 9,10-(●), or 11,12Br_2-PC (▲) containing (X = 0.3) LUV. The latter was composed of POPC (panels A & B), CL/POPC ($X_{CL} = 0.2$, panels C & D), and POPS/POPC ($X_{POPS} = 0.2$, panels E & F) LUV. The quenching efficiencies are depicted as the ratio of relative fluorescence intensities with LUV as such (F_0) and LUV with the indicated Br_2PCs (F), data measured at pH 7.4 (lefthand panels), or pH 6.0 (righthand panels).

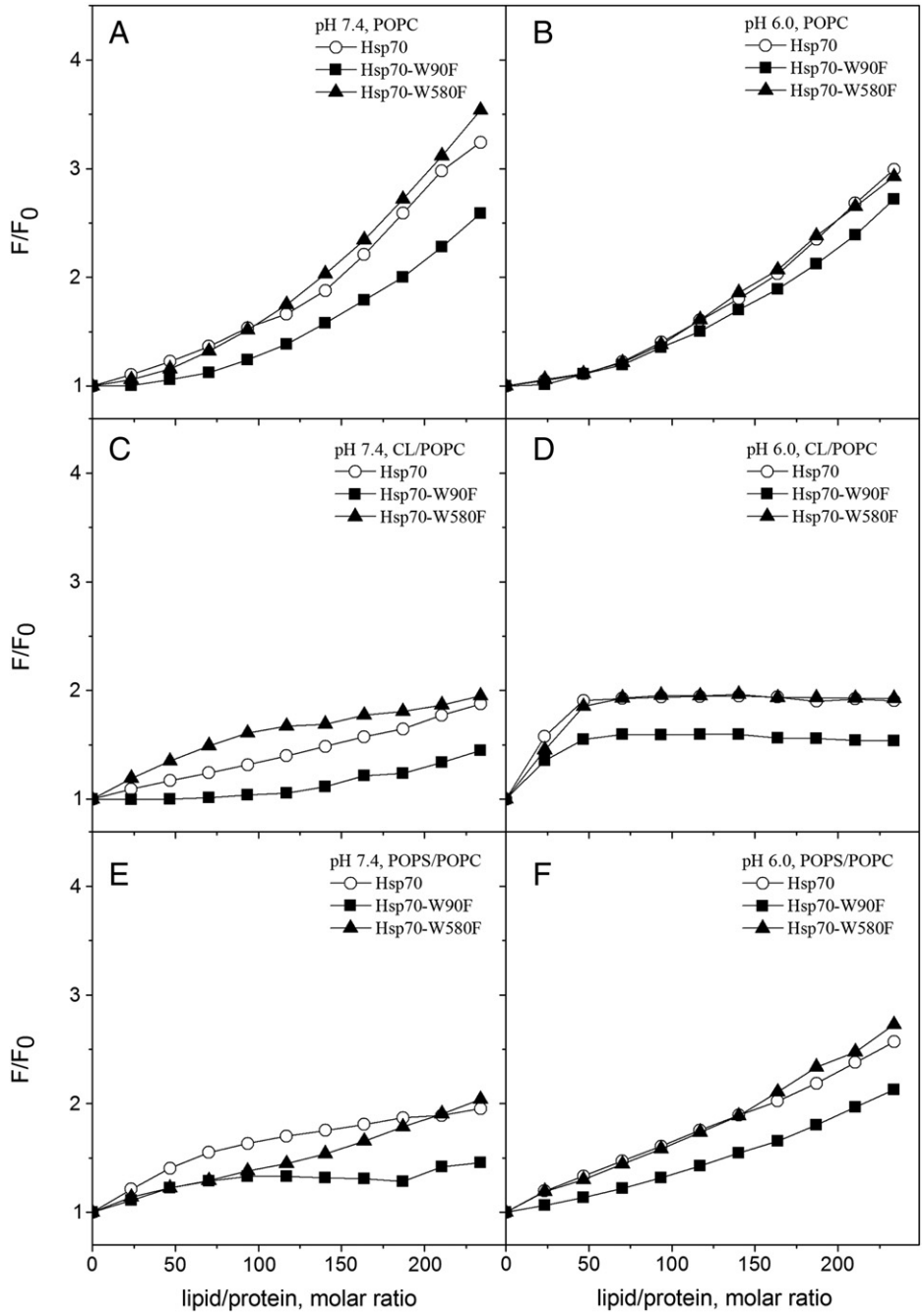

Fig. 5. Relative fluorescence intensities for Hsp70 (○), Hsp70-W90F (W580, ■), and Hsp70-W580F (W90, ▲) in the presence of POPC (panels A & B), CL/POPC (X_{CL} = 0.2 panels C & D), and POPC/POPS (X_{POPS} = 0.2, panels E & F) LUV. Initial protein concentration was 0.43 μM and the concentration of lipid was increased in 10 μM increments. The data are depicted as the ratio (F/F_0) of the emission measured in the presence of the indicated LUV (F) and the emission intensity in 20 mM Hepes, 0.1 mM EDTA (F_0) at pH 7.4 (lefthand panels), or pH 6.0 (righthand panels).

LUV at pH 6.0 (Fig. 8, panel B), supporting the conclusion that W90 in NBD contacts bilayer hydrocarbon region, while W580 in SBD still remains accessible also to the bulk aqueous phase (Fig. 8, panel B).

Lipid monolayers (Langmuir-films) residing on a gas/water interface provide an excellent model to study protein–lipid interactions and protein penetration into membranes under highly controlled conditions. Lipid lateral packing density in monolayers can be precisely adjusted, which allows the extent of the insertion of Hsp70 into the film to be investigated as a function of the initial value π_0. As an independent check for a possible intercalation of Hsp70 into POPC membranes suggested by our Trp fluorescence data (*e.g.* experiments demonstrating significant quenching by brominated PCs included in POPC LUV), we measured the penetration of Hsp70 into POPC monolayers residing on an air/buffer interface, at a range of initial lateral pressures (Fig. 9, panels A & B). The equilibrium lateral pressures estimated for biomembranes are approximately 33–35 mN/m [47]. The exclusion pressures π_c of 47 and 38 mN/m, measured for Hsp70 and POPC monolayers at pH 7.4 and 6.0, respectively, demonstrate that Hsp70 can efficiently incorporate into PC films, at neutral pH, in particular. The intercalation of Hsp70 into POPC monolayers is reduced at pH 6.0, again in keeping with results from Trp fluorescence.

3.1.2. Binding of Hsp70 to liposomes containing cardiolipin

Judged from Trp fluorescence the binding of Hsp70 to CL/PC (X_{CL} = 0.2) LUV (Fig. 3, panel F) resembles that described previously by us for BMP/PC bilayers [30]. Lower RFI in the spectra for CL containing

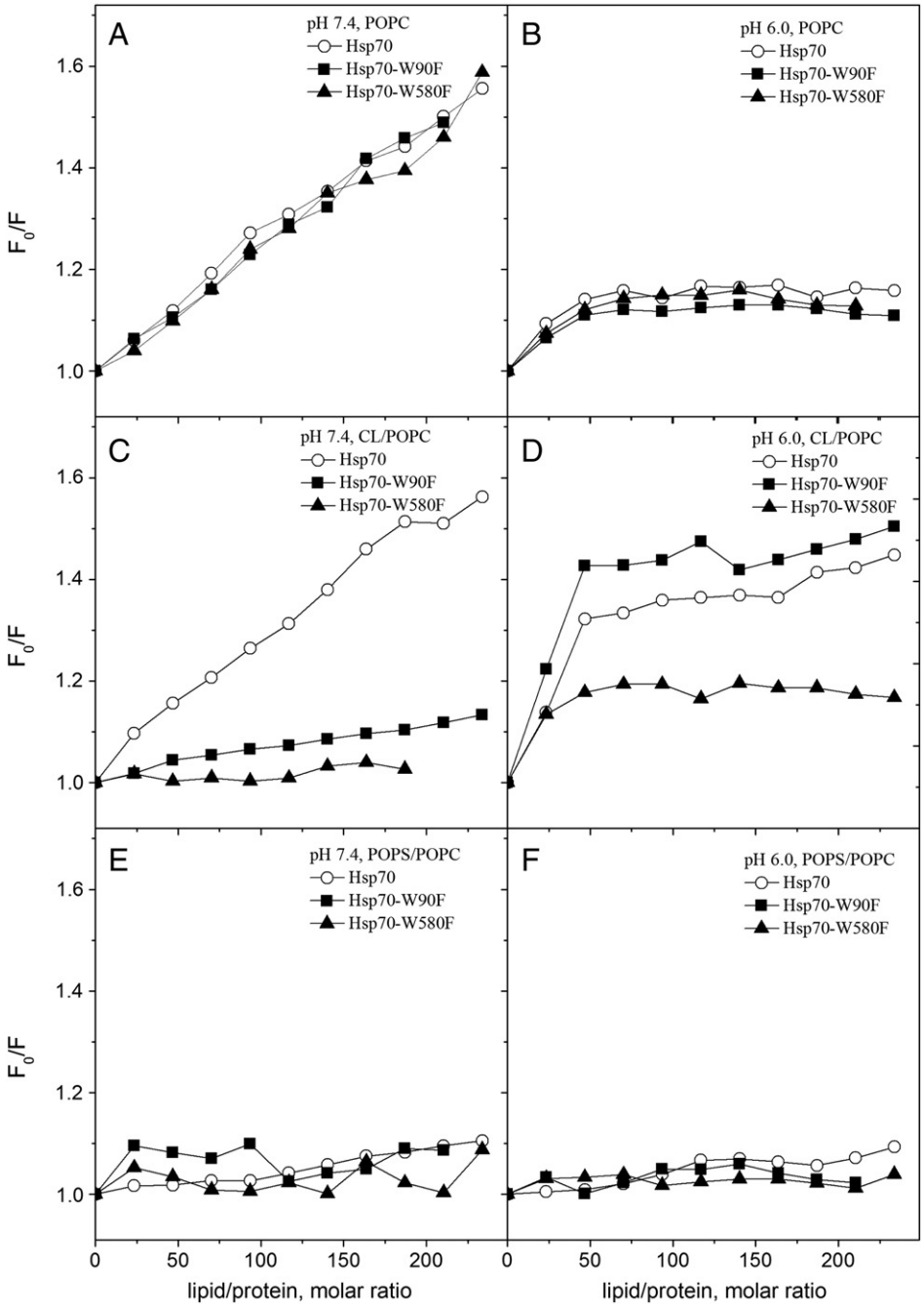

Fig. 6. Quenching by 6,7Br_2-PC (X = 0.3) of Hsp70 (○), Hsp70-W90F (W580, ■), and Hsp70-W580F (W90, ▲) Trp fluorescence in POPC (panels A & B), CL/POPC (X_{CL} = 0.2, panels C & D), or in POPS/POPC (X_{POPS} = 0.2, panels E & F) LUV. The quenching efficiencies are depicted as the ratio of relative fluorescence intensities with liposomes as such (F_0) and LUV with 6,7-Br_2PC (F), measured at pH 7.4 (lefthand panels), or pH 6.0 (righthand panels).

LUV compared to POPC could reflect the vicinity of the Trps to the surface charges of CL/PC liposomes (Fig. 3). No significant differences in the values of λ_{max} were seen for spectra recorded between pH 7.4 and 6.0 with CL/PC (X_{CL} = 0.2) liposomes (Fig. 3, panels C & D), although at pH 6.0 the overall values for RFI were approx. 26% higher (Fig. 3, panels A & B).

The significant quenching of Hsp70 by 11,12-Br_2PC in the presence of cardiolipin at pH 7.0 reveals that the Trps are in contact with the *sn*-2 acyl chain of PC (Fig. 4, panel C). Binding of Hsp70 to CL-containing liposomes with brominated PCs (Fig. 4, panel D) at pH 6.0 reveals efficient quenching with similar dependence on L/P as seen for the Trp emission of Hsp70 in the presence of CL/PC LUV, with saturation observed at L/P ≈ 50 (Fig. 3, panel F). Accordingly, at pH 6.0 the affinity of Hsp70 to CL/POPC LUV seems to be high (Fig. 4, panel D). This behavior was observed neither for POPC (Fig. 4, panels A & B) nor for POPS/POPC LUV (see below). Of the brominated PCs, the 6,7-Br_2-PC caused the most efficient quenching and was thus selected for subsequent experiments.

Compared to wtHsp70 the affinities for CL of the W90F and W580F mutants seem to be different, saturating at approx. L/P ≈ 50, and 75, respectively (Fig. 5, panel D). Accordingly, both NBD and SBD contribute to the attachment of Hsp70 with CL containing bilayer. The membrane affinity of the NBD domain appears to be slightly reduced by the W580F mutation in SBD, in keeping with a conformational coupling

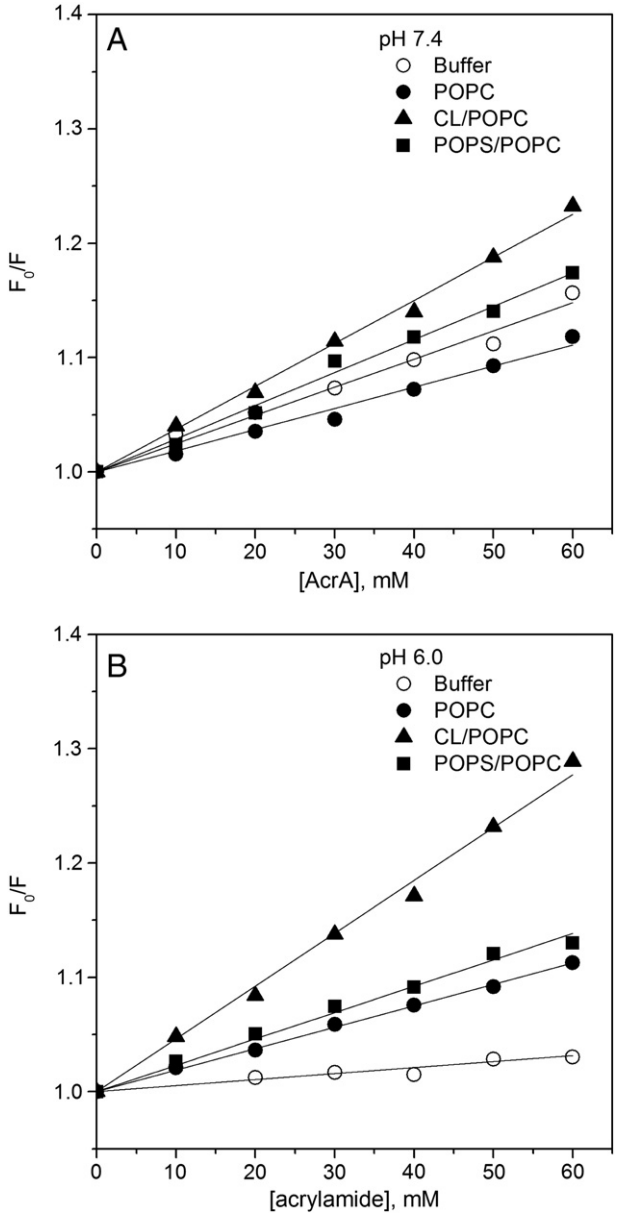

Fig. 7. Quenching by AcrA of Trp fluorescence of membrane bound Hsp70. The concentrations of lipids and Hsp70 were 95 and 0.4 μM, corresponding to L/P ≈ 234. The data are represented as the ratio of initial fluorescence intensity (F_0) and the intensity measured in the presence of AcrA (F), at pH 7.4 (panel A) and 6.0 (panel B). The liposomes were composed of POPC (●), CL/POPC ($X_{CL} = 0.2$, ▲), and POPS/POPC ($X_{POPS} = 0.2$, ■). Also shown are data for Hsp70 in buffer (○). Although the depicted results were from a single experiment, these data were readily reproducible and consistent in all similar experiments (data not shown).

between the two domains. Efficient quenching of W580 in the Hsp70-W90F mutant by 6,7-Br_2PC in CL/POPC LUV revealing a high affinity interaction of the SBD domain with CL/PC LUV (Fig. 6, panel D), suggests that SBD possesses a high affinity binding site for CL.

Interestingly, at both pH 7.4 and 6.0, the binding of Hsp70 to CL/PC bilayers results in an augmented quenching by AcrA (Fig. 7), at acidic pH in particular, indicating a conformational change which renders at least one of the Trp residues in Hsp70 more exposed to water. This is in keeping with a red shift which is evident in the fluorescence spectrum of the Trp residue, which is not contacting the brominated acyl chains of PCs (Table 1), suggesting that at least one of the Trp residues remains accommodated in a more hydrophilic environment in the presence of CL/PC LUV. Interestingly, compared to Hsp70, there is attenuated quenching of Hsp70-W90F and Hsp70-W580F Trp fluorescence by AcrA (Fig. 8, panel D), suggesting that both domains are required for the opening of the Hsp70 structure when bound to CL.

Importantly, the association of Hsp70 with CL/PC monolayers is distinctly different from that with POPC, with π_0 *vs* $\Delta\pi$ data revealing low exclusion pressures π_e of 27.5 and 31 mN/m, respectively, at pH 7.4 and 6.0 (Fig. 9). Lack of increment in the surface pressure of CL/PC monolayers at the above initial surface pressures following the injection of the Hsp70 into the subphase suggests a lack of intercalation of Hsp70 into CL/PC bilayer, estimated to have lateral pressure of approximately 33–35 mN/m [47].

To further explore the interactions of CL with the Hsp70 domains we used brominated toCL (Br_8CL). The efficient quenching of Hsp70 Trps by Br_8CL at pH 7.4 reveals that the Trps are in direct contact with the CL acyl chain bromides (Fig. 10, panel A). Quenching of wtHsp70 at pH 6.0 reveals a high affinity interaction, saturating at L/P ≈ 30 (Fig. 10, panel B). For $X_{CL} = 0.2$ this corresponds to CL/P ≈ 6. Assuming uniform distribution of CL in the two leaflets of the LUV bilayers the number of CL reacting with Hsp70 is close to 3:1. The efficient quenching for both Hsp70-W580F and Hsp70-W90F by Br_8CL at pH 6.0, saturating at approx. L/P ≈ 50 and 100, respectively, shows that both NBD and SBD contain CL binding sites (Fig. 10, panel B). These interactions with CL further result in direct contacts of the brominated acyl chains of CL and W90 and W580. Yet, the affinity of Hsp70 to the above CL/PC bilayers is significantly reduced by both W90F and W580F mutations, again in keeping with a conformational coupling of the two domains.

The far-UV CD spectra of 2 μM Hsp70 in 20 mM MES, 0.1 EDTA at pH 6.0 show double minimum at 222 and 210 nm (Fig. 11, panel A) characteristic to a protein containing predominantly α-helical structure. The calculated helical content decreased slightly, from 84 to 83% by the presence of CL/POPC ($X_{CL} = 0.2$) LUV, suggesting CL-containing membrane induce a minor change in the overall secondary structure of Hsp70. Yet, near UV-CD of Hsp70 in the presence CL/POPC ($X_{CL} = 0.2$) LUV indicates loss of asymmetry in the aromatic environment (Fig. 11, panel B), in keeping with molten globule state.

3.1.3. Binding of Hsp70 to liposomes containing bis-monoacylglycero phosphate

In order to relate the above data to our earlier results for the interaction of Hsp70 with BMP, we additionally investigated the binding at pH 6.0 of Hsp70 to PC LUV containing BMP, or brominated BMP (Br_4BMP), or Br_2PCs (Fig. 12). For BMP/POPC ($X = 0.2$) quenching by Br_2PCs is seen, saturating at L/P ≈ 30, similarly to CL/PC LUV (Fig. 12, panel A). Likewise, quenching by Br_4BMP ($X = 0.2$) saturates at this stoichiometry (Fig. 12, panel B). Most efficient quenching by Br_4BMP is seen for W90, in keeping with the suggested binding site for this lipid in NBD [30].

Binding to BMP/PC LUV and quenching of Hsp70 by Br_2PCs (Fig. 12, panel A) at pH 6.0 reveal only weak quenching. In keeping with the weak quenching by Br_2PCs and the observed red shift in the fluorescence spectrum (Table SI), Hsp70 does not seem to penetrate into BMP/PC bilayers and at least one of the Trp residues becomes accommodated in a more hydrophilic environment in the presence of BMP/PC LUV. To further explore the BMP–Hsp70 interactions we used Br_4BMP. Quenching of wtHsp70 at pH 6.0 reveals a high affinity binding, saturating at L/P ≈ 30 (Fig. 12, panel B). The efficient quenching of both Hsp70-W580F and Hsp70-W90F by Br_4BMP contained in BMP/PC LUV and at pH 6.0, both saturating at approx. L/P ≈ 30, suggests that there are binding sites for BMP in both NBD as well as SBD (Fig. 12), similar to the observations on the binding of Hsp70 to CL/PC LUV. Langmuir films of BMP/PC gave an exclusion pressure of 27 mN/m at pH 6.0, indicating no intercalation into BMP/PC membranes (Fig. 9, panel B), estimated to have lateral pressure of approximately 33–35 mN/m [47].

Compared with buffer, the helical content calculated from CD spectra increased slightly, from 84 to 85% by the presence of BMP/POPC

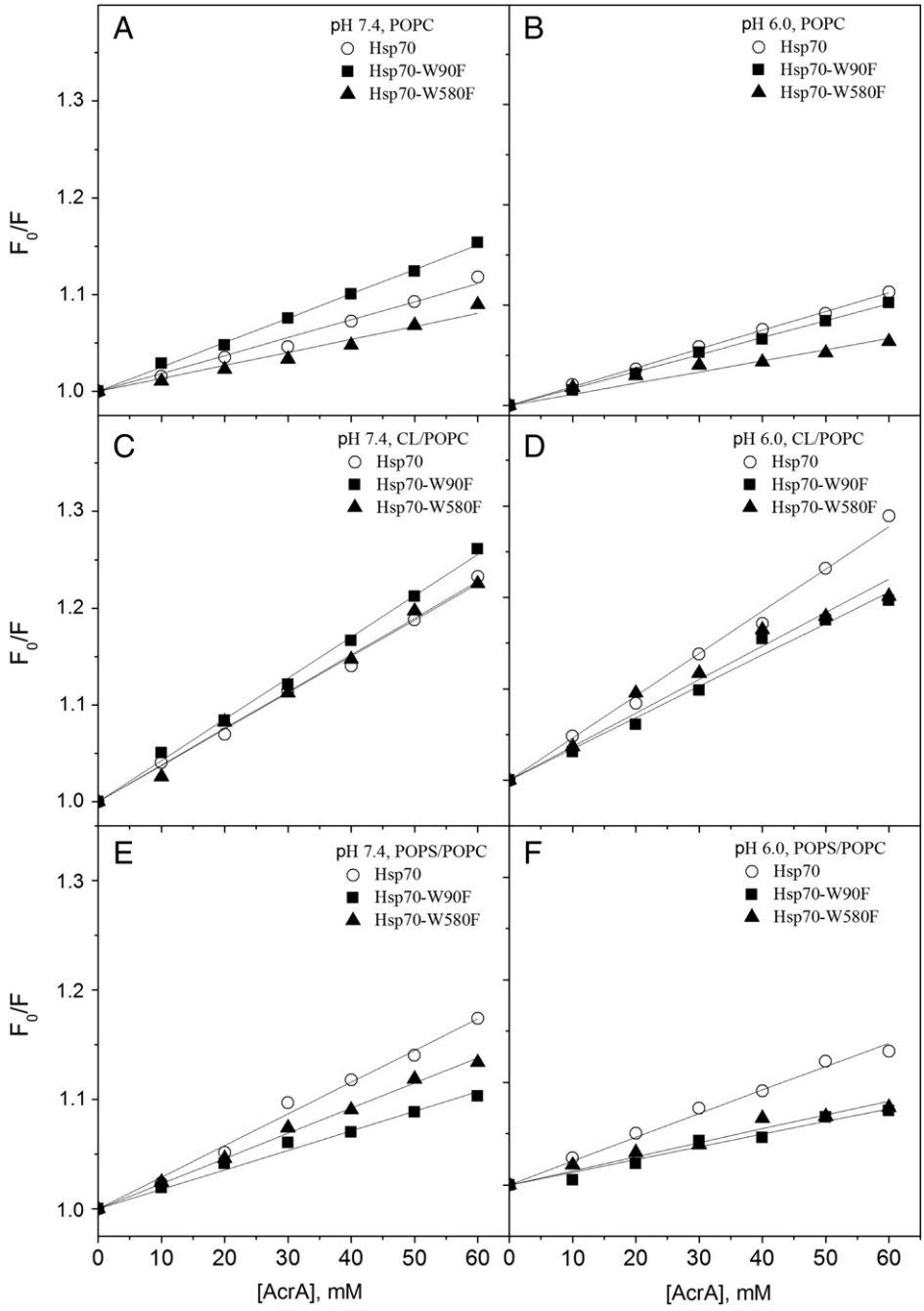

Fig. 8. AcrA quenching for Hsp70 (○), Hsp70-W90F (W580, ■), and Hsp70-W580F (W90, ▲) in the presence of POPC (panels A & B), CL/POPC (X_{CL} = 0.2, panels C & D), and POPS/POPC (X_{POPS} = 0.2, panels E & F) LUV. The concentrations of lipids and proteins were 95 and 0.4 μM, corresponding to L/P ≈ 234. The data are represented as the ratio of initial fluorescence intensity (F_0) and the intensity measured in the presence of increasing concentrations of AcrA (F), data measured at pH 7.4 (lefthand panels), or pH 6.0 (righthand panels).

LUV (X_{BMP} = 0.2, Fig. 13, panel A). Similar to CL/PC LUV near UV-CD of Hsp70 in the presence BMP/POPC LUV (X_{BMP} = 0.2) indicates loss of asymmetry in the aromatic environment (Fig. 13, panel B), suggesting the molten globule state.

3.1.4. Binding of Hsp70 to liposomes containing phosphatidylserine

We then proceeded to study the interaction of Hsp70 with membranes containing the acidic phospholipid PS. Compared to neat POPC LUV, PS/PC LUV (X_{PS} = 0.2) also cause an increase in RFI, yet with a smaller decrement in λ_{max} (Fig. 3). This could reflect vicinity of W90 and W580 to the surface charges of the bilayers, similar to CL/PC LUV with almost identical spectra seen at pH 7.4 for the PS and CL containing membranes (Fig. 3). No significant differences in the values of λ_{max} were seen for the spectra recorded with PS/PC LUV at pH 7.4 and 6.0 (Fig. 3, panels C & D). At pH 6.0 the values for the emission band RFI increased and the peak was observed at a somewhat shorter λ_{max}. Compared to POPC LUV the changes in fluorescence induced by PS/PC LUV were more rapid and apparent equilibria were reached faster.

In contrast to POPC LUV, judged from the lack of significant quenching by the brominated PCs Hsp70 does not insert into PS containing membranes (Fig. 4, panels E & F).

Judged from relative fluorescence intensities both Hsp70-W90F and Hsp70-W580F seem to be involved in interactions with PS containing membranes (Fig. 5, panels E & F). The lack of quenching by 6,7-Br_2PC reveal that neither NBD nor SBD insert into PS containing membranes (Fig. 6, panels E & F).

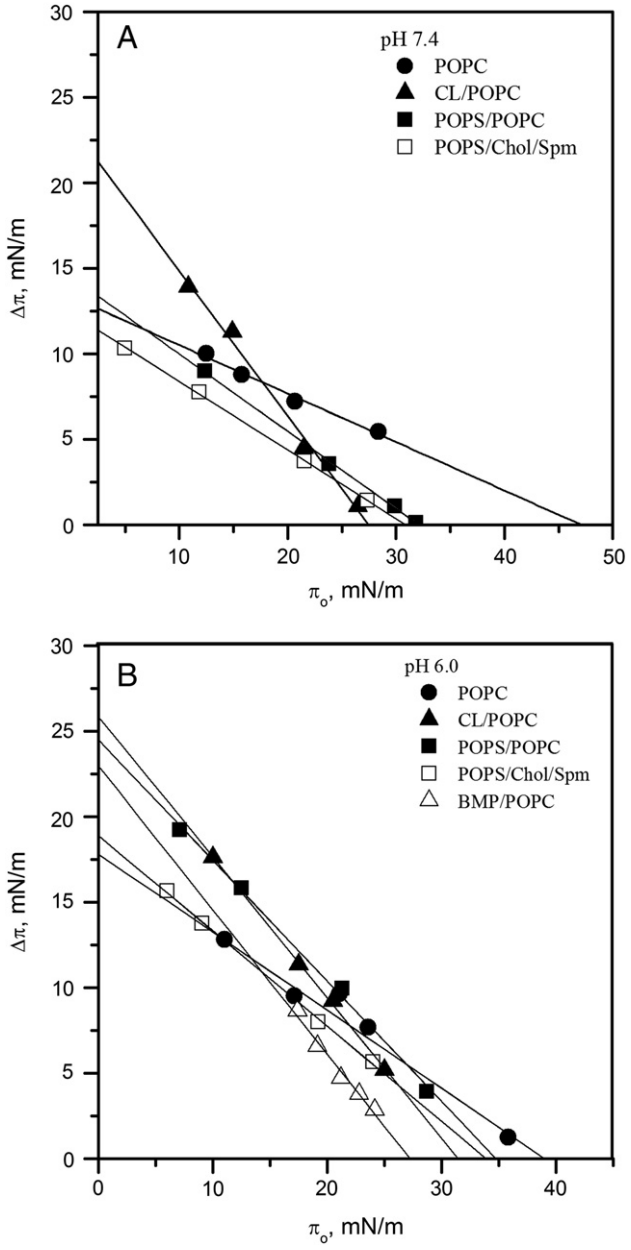

Fig. 9. Penetration of Hsp70 into lipid monolayers residing on 20 mM Hepes, 0.1 mM EDTA at pH 7.4 (panel A) or 6.0 (panel B), illustrated as a function of the initial surface pressure π_0 and the increment in surface pressure ($\Delta\pi$) following the injection of Hsp70 into the subphase (0.1 μM final concentration). Lipid monolayers were POPC (●), CL/POPC ($X_{CL} = 0.2$, ▲), POPS/POPC ($X_{POPS} = 0.2$, ■), POPS/Chol/Spm ($X_{POPS} = 0.10$, $X_{Chol} = X_{Spm} = 0.45$, □), and BMP/POPC ($X_{BMP} = 0.2$, Δ).

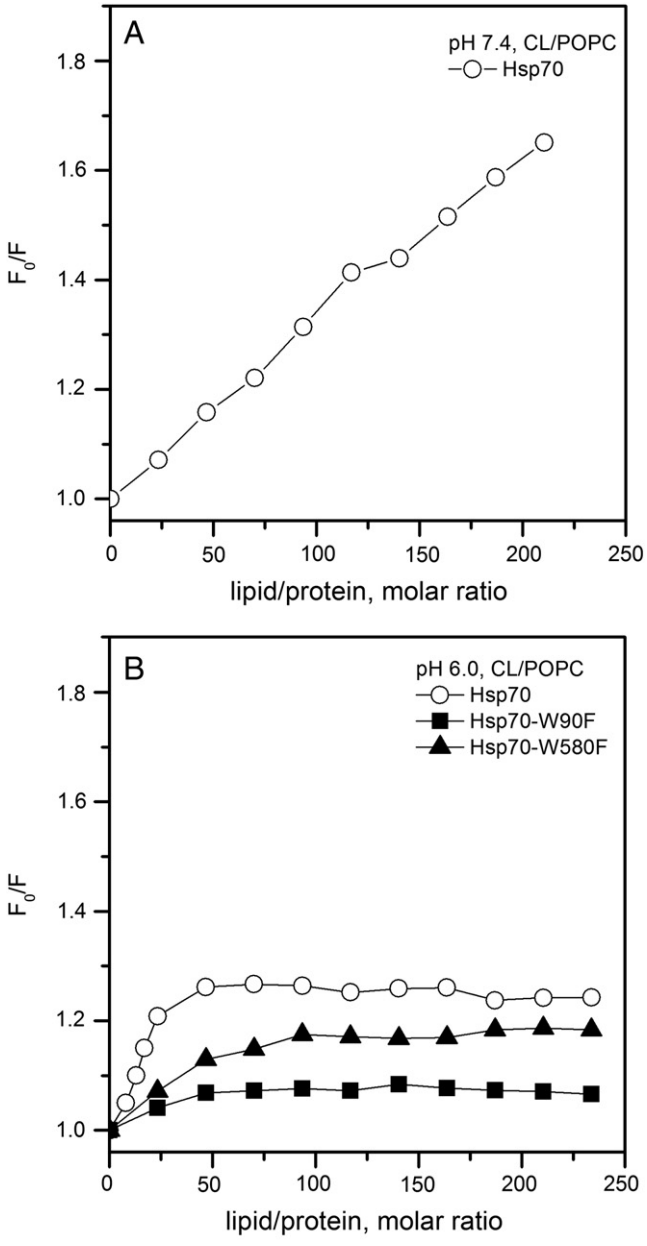

Fig. 10. Quenching of Hsp70 Trps (○) by Br_8CL ($X = 0.2$, in CL/POPC LUV) at pH 7.4 (panel A) as well as Hsp70 (○), Hsp70-W90F (W580, ■), and Hsp70-W580F (W90, ▲) at pH 6.0 (panel B). Quenching efficiencies are depicted as the ratio of relative fluorescence intensities with LUV without (F_0) and with Br_8CL (F). Initial concentration of the proteins was 0.43 μM while the concentrations of lipids were increased in 10 μM (total lipid) increments.

The above aligns with the efficient quenching of Hsp70 Trps seen for AcrA in the presence of PS/PC LUV, revealing that the Trps remain accessible to the bulk aqueous phase (Fig. 7, panels A & B). However, this contradicts the reduced quenching of W90F and W580F by AcrA in the presence of PS/PC LUV, suggesting shielding of the Trps from access to AcrA in the bulk aqueous phase for these mutants (Fig. 8, panels E & F).

PS/PC Langmuir films gave for Hsp70 exclusion pressures of 33 and 35 mN/m at pH 7.4 and 6.0, respectively, suggesting only weak intercalation into PS/PC membranes to be possible (Fig. 9). For sphingomyelin/cholesterol (1/1, molar ratio) films with 10 mol% PS exclusion pressures of 31 and 34 mN/m at pH 7.4 and 6.0, respectively, were recorded, thus suggesting a lack of significant protein intercalation into lipid films corresponding to those found in the plasma membrane of cancer cells.

The lack of quenching of Trps by Br_2PCs contained in PS/PC LUV could indicate that PS is displacing the brominated PCs from their binding sites in Hsp70 (Fig. 6, panels E & F). In keeping with binding of PS to Hsp70 is an efficient quenching of Trp emission by Br_2PS was observed (Fig. 14, panels A & B). Further, the quenching of both Hsp70-W90F and Hsp70-W580F Trps by Br_2PS at pH 6.0, both saturating at approx. L/P ≈ 100 and 50, respectively, suggests that both NBD as well as SBD contained binding sites for PS (Fig. 14, panel B).

3.2. Domain-specific lipid interactions of Hsp70

In the second part of this study we aimed at the identification of possible different interactions of the two domains (NBD & SBD) of Hsp70

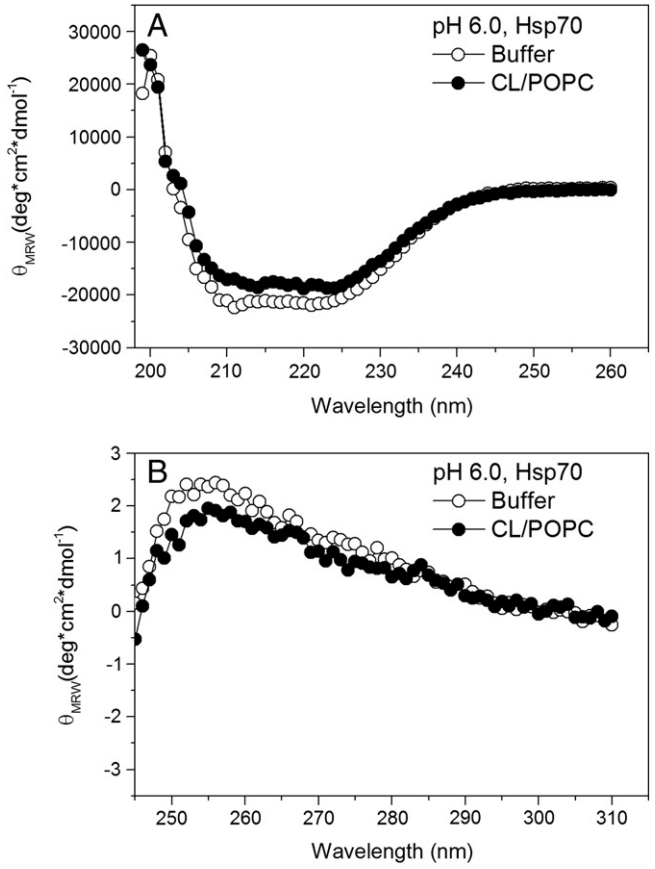

Fig. 11. Panel A: Far-UV CD spectra of 2 μM Hsp70 (○) in buffer (20 mM MES, 0.1 EDTA) and in the same buffer in the presence of 200 μM (total lipid) CL/PC (X_{CL} = 0.2, ●) LUV at pH 6.0. Panel B: Near-UV CD spectra of 8.5 μM Hsp70 (○) in buffer (20 mM MES, 0.1 EDTA) and in the same buffer in the presence of 700 μM (total lipid) CL/PC (X_{CL} = 0.2, ●) LUV at pH 6.0.

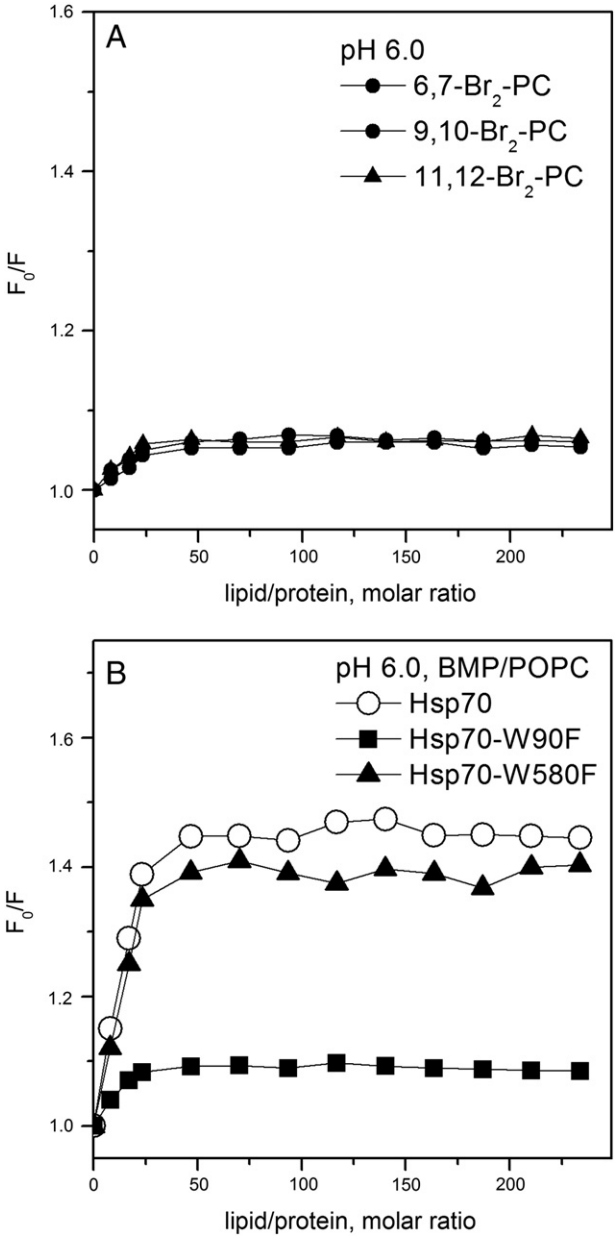

Fig. 12. Quenching of Hsp70 Trp fluorescence by 6,7-(■), 9,10-(●), or 11,12Br_2-PC (▲, X = 0.3) contained in BMP/POPC (X_{BMP} = 0.2) LUV at pH 6.0 (panel A). Quenching of Hsp70 (○), Hsp70-W90F (W580, ■), and Hsp70-W580F (W90, ▲) Trp fluorescence by Br_4BMP (X = 0.2, in POPC LUV) at pH 6.0 (panel B). The quenching efficiencies are depicted as the ratio of relative fluorescence intensities with LUV without (F_0) and with the brominated lipid (F), as indicated.

with the above three different phospholipids, employing the constructs Hsp70-ΔNBD, and Hsp70-ΔSBD, lacking NBD and SBD, respectively (Fig. 1, panel B). Unfortunately, the former construct also contains part of the NBD (residues 1 to 118, including W90) as attempts to delete this domain completely resulted in an expression product prone to extensive aggregation. The latter property of SBD has been observed previously in other laboratories [48]. Comparison of the spectra of Hsp70 and the above constructs reveals that the emission from the single Trp containing NBD construct is insensitive to buffer pH (Fig. S1). Changes in fluorescence recorded in the presence of LUV composed of POPC, as well as CL in POPC, or PS in POPC (as indicated) reveal that both constructs retain the ability to interact with phospholipid bilayers.

Comparison of the quantum yields of Hsp70 and the above Trp → Phe mutants reveals conformational coupling between the NBD and SBD. For example, the combined emission of Hsp70-ΔSBD and Hsp70-ΔNBD at L/P ≈ 230 exceeds the intensity of wtHsp70 fluorescence (Fig. S2).

POPC LUV induced, similar to Hsp70, profound changes in Trp fluorescence of both Hsp70-ΔSBD, and Hsp70-ΔNBD (Fig. S3, panels A & B), with a large increase in the relative fluorescence intensity values (RFI) indicating a major change (increase) in the hydrophobicity in the surroundings of their Trp residues. Interactions of NBD and SBD with PC seem to be non-specific and of low affinity. The fluorescence enhancement induced in the presence of PC LUV is larger for NBD than for SBD, which contains two Trps, and thus supports our earlier conclusion that in wtHsp70 it is the NBD and its W90 which insert into PC bilayers.

Compared to wtHsp70 the affinity of the NBD construct for CL appears to be reduced, whereas for SBD and CL a high affinity interaction is evident, saturating at approx. L/P ≈ 50 (Fig. S3, panel D). Judged from relative fluorescence intensity values both NBD and SBD seem to be involved in interactions with membranes containing PS (Fig. S3, panels E & F). Interestingly, both NBD and SBD contribute to the bilayer attachment of Hsp70.

The quenching of Hsp70-ΔNBD and Hsp70-ΔSBD Trps by Br_2-6,7PC contained in POPC LUV suggests that Hsp70 penetrates into POPC LUV (Fig. S4, panels A & B). Similar to the above, efficient quenching of Hsp70-ΔNBD and Hsp70-ΔSBD Trps by Br_2-6,7PC is observed with CL/PC LUV ($X_{Br2\text{-}6,7PC}$ = 0.2, Fig. S4, panels C & D). The lack of quenching of Hsp70-ΔNBD and Hsp70-ΔSBD Trps by Br_2PCs contained in PS/PC LUV suggests that PS is displacing the brominated PCs from their binding sites in Hsp70 (Fig. S4, panels E & F).

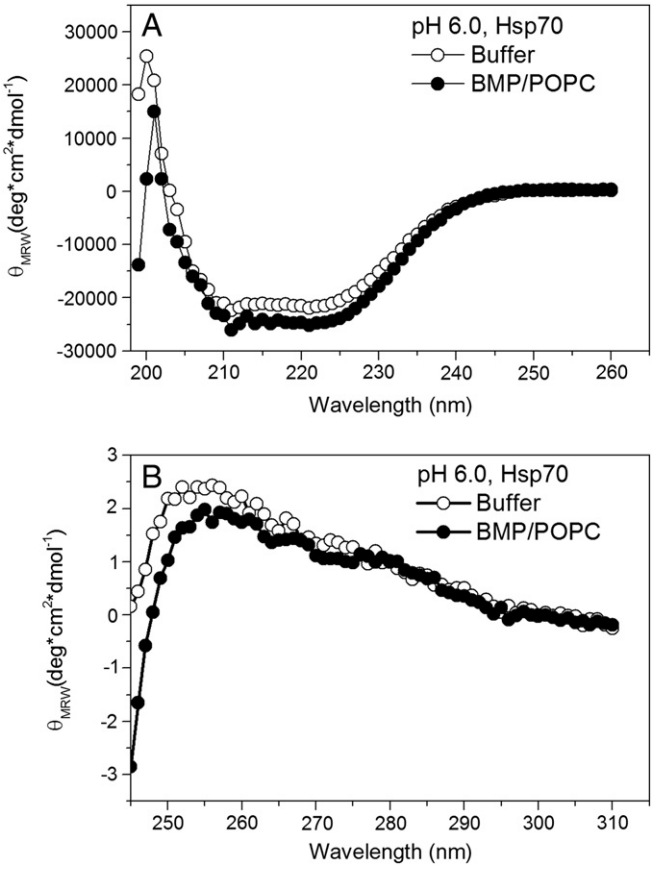

Fig. 13. Panel A: Far-UV CD spectra of 2 μM Hsp70 (○) in buffer (20 mM MES, 0.1 EDTA) and in the same buffer in the presence of 200 μM (total lipid) BMP/PC (X_{BMP} = 0.2, ●) LUV at pH 6.0. Panel B: Near-UV CD spectra of 8.5 μM Hsp70 (○) in buffer (20 mM MES, 0.1 EDTA) and in the same buffer in the presence of 700 μM (total lipid) BMP/PC (X_{BMP} = 0.2, ●) LUV at pH 6.0.

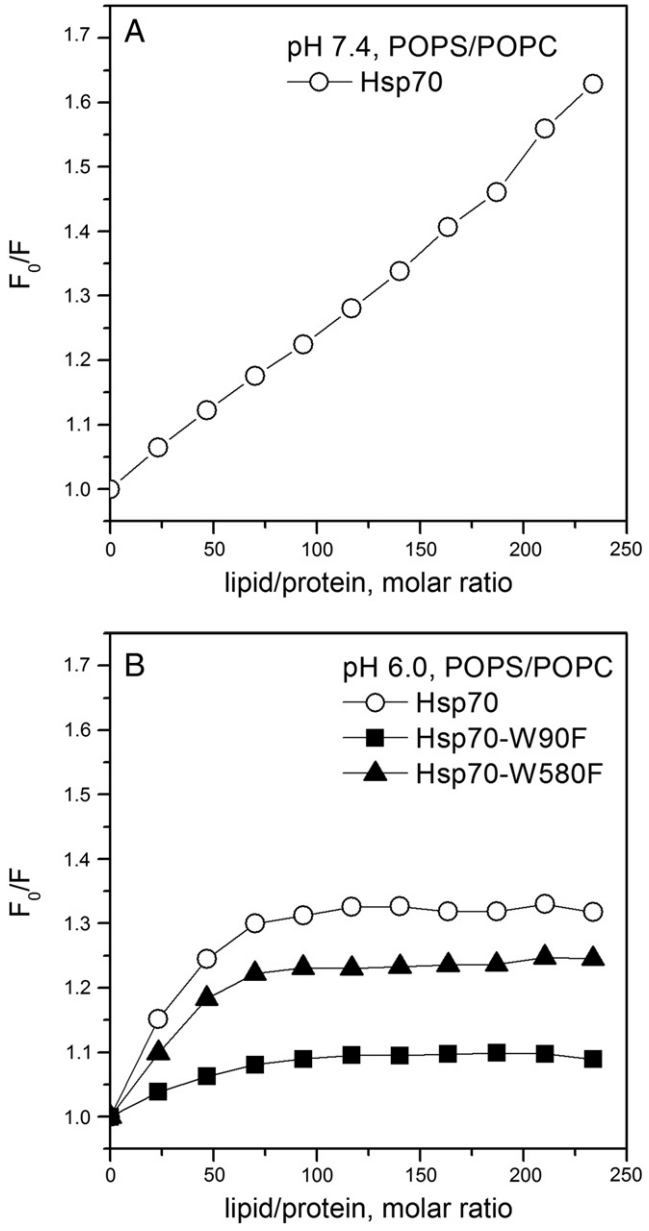

Fig. 14. Panel A, Quenching of Hsp70 Trps (○) by Br_2PS (X = 0.2, in PS/POPC LUV) at pH 7.4, and panel B at pH 6.0 Hsp70 (○), Hsp70-W90F (W580, ■), and Hsp70-W580F (W90, ▲). Quenching efficiencies are depicted as the ratio of relative fluorescence intensities with LUV with PS (F_0) and Br_2PS (F). Initial concentration of the proteins was 0.43 μM while the concentration of lipids was increased in 10 μM increments.

At both pH 7.4 and 6.0, augmented quenching of Hsp70-ΔNBD Trp emission by AcrA is seen upon binding to CL/PC LUV, suggesting a conformational change, which opens the structure of SBD, enhancing the exposure and access of AcrA to W580 (Fig. S5, panels C & D). In contrast, less efficient quenching of Hsp70-ΔSBD W90 by AcrA was evident at both pH, suggesting that W90 was buried inside NBD in a more compact structure when bound to CL/PC membranes (Fig. S5, panel D). At both pH 7.4 and 6.0, augmented quenching of Hsp70-ΔNBD Trp in the presence of PS/PC LUV by AcrA is evident, suggesting a conformational change, which opens the structure of SBD making W580 more exposed to water (Fig. S5, panels E & F). In contrast, less efficient quenching of Hsp70-ΔSBD W90 in the presence of PS/PC LUV by AcrA was seen at both pH 7.4 and 6.0, suggesting that W90 becomes buried inside NBD folded into a compact structure when bound to PS/PC membranes (Fig. S5, panel F), similar to the data measured in the presence of CL/PC LUV.

4. Discussion

Studies on the interaction of Hsp70 with lipid membranes are sparse and have been mainly limited to qualitative observations. We describe here a somewhat more detailed assessment of the binding of Hsp70 to specific lipids. Our previous results demonstrated that BMP could represent the membrane ligand responsible for the localization of Hsp70 in the lysosomal/endosomal membranes, required for the cytoprotective effect of Hsp70, resulting from the activation of acidic sphingomyelinase and subsequent formation of ceramide. In this study we investigated if Hsp70 would exhibit similar specific interactions with other acidic phospholipids. Importantly, due to the limited availability of the Hsp70 protein and the constructs, we focused at this stage for first obtaining a qualitative view on the mechanisms on Hsp70–lipid interactions, in order to provide a good starting point for possible later quantitative analyses.

Regarding the association of Hsp70 with different lipids, the following conclusions could be made,

(i) Hsp70 associates with POPC bilayers, with shallow penetration into the membrane. W90 in NBD appears to signal this penetration, and resides at a distance of approximately 11 Å from the bilayer center, in the interfacial region of the bilayer and still also accessible to weak collisional quenching by the water soluble AcrA. At pH 6.0 the penetration of Hsp70 into POPC is less than at pH 7.4, evidenced by both Trp fluorescence as well as Langmuir-film penetration experiments.

(ii) The presence of CL has a profound impact on the membrane association of Hsp70. The interaction between CL and Hsp70 at pH 6.0 seems to be of high affinity and abolishes the penetration of Hsp70 into CL/PC Langmuir films. Taken together our data on the binding of Hsp70 to CL/PC membranes suggest that CL adopts the extended conformation, thus anchoring Hsp70 to the lipid surface [33,34].

In keeping with earlier observations, Hsp70 binds avidly to liposomes containing negatively charged lipids [30,31]. The effects of LUV with different lipid compositions correlate with the structure of the acidic phospholipid headgroup. Insignificant changes in the net charges of POPC, POPS, and CL, *viz.* 0, −1, and −2, respectively, are anticipated upon decreasing pH from 7.4 to 6. In contrast, for Hsp70 net charges of −10.9 and −3.5 at pH 7.4 and 6.0, respectively, can be estimated. The corresponding values for NBD are −4.8 and +1.0, and for SBD −9.1 and −5.5 (at pH 7.4 and 6, respectively). These charges of Hsp70 and its two domains should, however, be taken as tentative only as they were calculated based on the amino acid sequence, neglecting any effects of protein three-dimensional structure, schematically illustrated in (Fig. 1, panel A). From the point of view of electrostatic interactions with anionic lipids, it is of interest that both NBD and SBD expose on their surface positively charged residues. At pH 7.4 Hsp70 binds to negatively charged liposomes in a rather similar manner irrespective of the acidic phospholipid species present (Figs. 3 and 5). This may be explained by the net negative charge of the protein and its both domains at pH 7.4 causing repulsion between Hsp70 and the negatively charged membranes. Lowering pH to 6.0 changes the estimated net charge of NBD from negative to positive (−4.8 to +1.0), which could explain the altered membrane binding (Fig. 3). With respect to the pH dependence of the lipid binding of Hsp70 as reflected in Trp fluorescence, the roles of His89 and 594 are of interest, being vicinal to W90 and W580, respectively [49].

We assessed possible specific lipid interactions of Hsp70 by using W90 and W580 as intrinsic fluorescent probes. At this point it is important to bear in mind the caveats involved. Accordingly, interpretation of the Trp fluorescence data for wtHsp70 is complicated by the presence of the two Trps (in NBD and SBD), in particular with the conformations of these two domains being coupled [7]. Moreover, both W90F and W580F mutations are readily reflected in the structural dynamics of native SBD and NBD, respectively (Figs. 5 and 14), in keeping with their conformational coupling. Likewise, the fact that the mutation W90F renders Hsp70 inactive [30] may also mean that the perturbation that caused this mutation in NBD is also reflected in the conformational dynamics of SBD, resulting in its altered interactions with lipids. Of the phospholipids investigated POPC induced the most pronounced changes in Trp fluorescence. The slow stabilization of the changes in Trp emission upon binding to POPC requiring approx. 15–20 min indicates that what happens is more than simple non-specific association. The exponential increase in RFI upon surface dilution of Hsp70 could indicate dimer/oligomer dissociation in POPC bilayers, resulting in a more efficient membrane intercalation (Fig. 3, panels E and F). The shoulder seen in the spectra in the presence of POPC liposomes suggests that one of the Trps becomes accommodated in a more hydrophobic microenvironment while the environment of the other Trp remains more or less unaltered (Fig. 3). The linear component observed at pH 7.4 (Fig. 3, panel E) may be interpreted as binding, with the subsequent component at L/P > 150 representing a process associated with a reorganization of Hsp70 in the membrane surface upon its surface dilution. The exponential increase is accompanied with a blue shift of about 10 nm in the peak position and about 5 nm in the spectral center of mass, in keeping with at least one of the two Trps entering a more hydrophobic environment. AcrA quenching shows shielding of the two Trps in the presence of POPC LUV at pH 7.4 (Fig. 7, panel A). Overall, our results suggest that the Trp becoming immersed into POPC bilayers is W90. The above data together with the demonstration of Trp

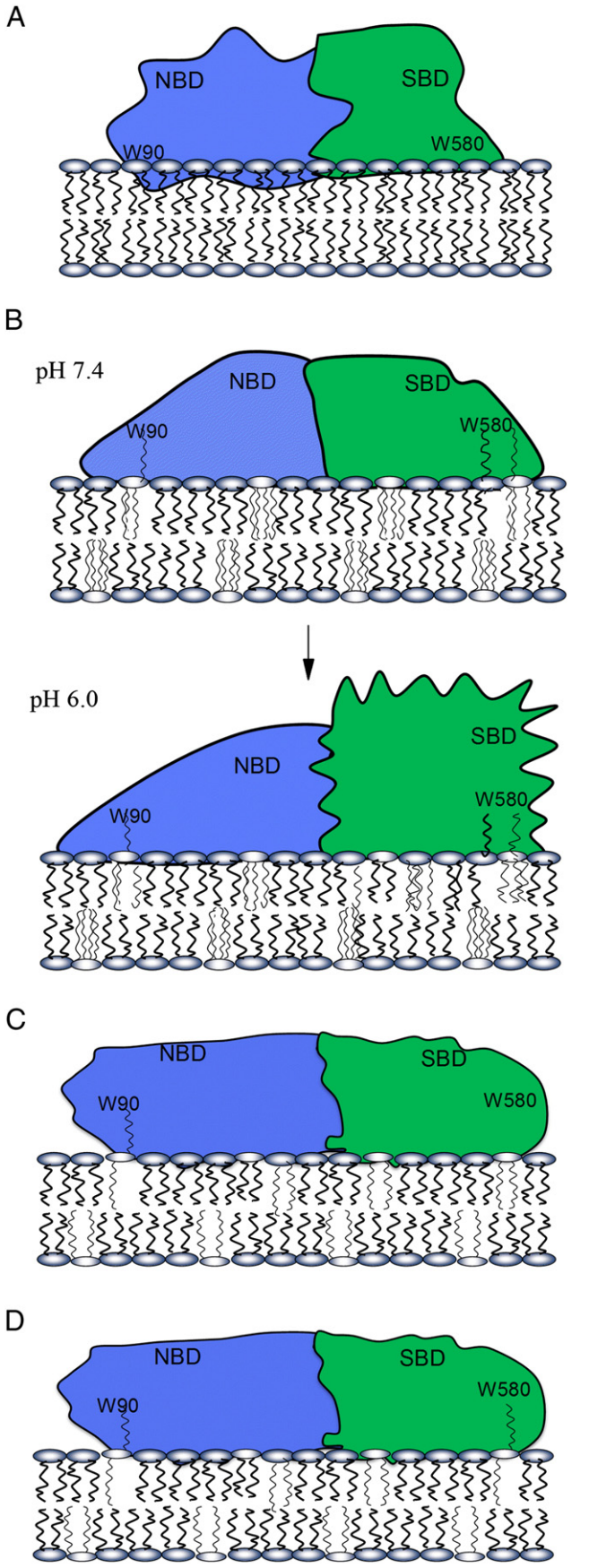

Fig. 15. Schematic illustration of the association of Hsp70 with POPC (panel A), CL/POPC (panel B), BMP/POPC (panel C), and POPS/POPC (panel D) membranes.

quenching by Br_2-PCs, suggest that Hsp70 penetrates into POPC LUV, in a manner (*i*) shielding access of AcrA to the Trps at pH 7.4, (*ii*) bringing W90 into a hydrophobic environment, and (*iii*) making W90 accessible to quenching by brominated PCs, 6,7Br_2-PC in particular. From parallax analysis the distance of the Trps quenched is approx. 11.4 Å from the bilayer center. The quenching of Hsp70-ΔNBD and Hsp70-ΔSBD Trps by Br_2-6,7PC (Fig. S4, panels A & B) together with Langmuir-film experiments (Fig. 9) comply with Hsp70 penetrating into POPC LUV. The interaction of Hsp70 with POPC membranes concluded on the basis of these data is schematically illustrated in Fig. 15 (panel A), in order to provide a plausible scenario to explain the experimental finding. Yet, considering the complexity of the molecular Hsp70 lipid bilayer assembly, the depicted arrangement needs to be taken at this time as tentative, not excluding other possible mechanisms.

Hsp70 indirectly blocks apoptotic pathways at premitochondrial and mitochondrial level, and also at a post-mitochondrial stage [50]. Hsp70 also mediates in an ATP dependent manner the translocation of proteins across the mitochondrial membrane, by the outer and inner membrane translocases [51,52]. Interestingly, Hsp70 protects mitochondria from damage by oxidative stress [53]. For Hsp70 acting in mitochondria the negatively charged cardiolipin would be likely to attach Hsp70 to the membranes of this organelle. The interaction of Hsp70 with CL/PC bilayers appears to be distinctly different from that with POPC liposomes. At pH 6.0 Hsp70 binds avidly to CL/POPC ($X_{CL} = 0.2$) liposomes with saturation seen at L/P ≈ 50 (Fig. 3, panel F). Notably, there is a red shift in the emission of W90 under these conditions, indicating a more polar environment, such as augmented exposure to water (Table 2). The two Trps of CL/PC bound Hsp70 are effectively quenched by AcrA, revealing that in the presence of CL/PC LUV the Trps become accessible for AcrA in the bulk aqueous phase. Nevertheless, these Trps are quenched also by brominated PCs, in keeping with an intercalation of Hsp70 into the bilayer. The association of Hsp70 with CL containing membranes is sensitive to pH, with a high affinity interaction being observed at pH 6.0 in a number of different experiments (Fig. 3, panel F; Fig. 4, panel D; Fig. 5, panel D, and Fig. 10, panel B). Our data point to a high affinity binding site for CL/PC membrane at acidic pH to be contained in SBD, as demonstrated by the quenching of W580 of Hsp70-W90F mutant by Br_2PCs (Fig. 6, panel D). Notably, because of the high content of protein in mitochondrial membranes the local content of cardiolipin is high, causing a high local negative surface charge, which necessarily attracts protons, generating a local low pH environment on the membrane surface [54,55]. Along these lines we previously demonstrated the membrane surface charge to have a dramatic influence on the pH dependence of the lipid association of cytochrome c [56].

Importantly, Hsp70 does not seem to intercalate into CL/PC monolayers at lipid packing densities corresponding to the equilibrium lateral surface pressures of approximately 33–35 mN/m estimated for biomembranes [47]. Intriguingly, this contradicts Trp quenching observed using brominated PCs as well as brominated CL. Interestingly, the efficient quenching of Hsp70-ΔNBD and Hsp70-ΔSBD Trps by Br_2-6,7PC contained in CL/PC LUV, with characteristics similar as seen for Hsp70 shows that both W90 & W580 in these constructs are contacting the brominated phospholipid acyl chains (Figs. 4–6, panel D). A likely mechanism to solve this paradox is that Hsp70 binds peripherally to the CL/PC bilayer surface, with the brominated phospholipid acyl chains adopting the so-called extended conformation [57,58] as first described by us for cytochrome c [33,34] and subsequently reported for bet3 [59] and Orf-9 [60]. This is schematically illustrated in Fig. 15 (panel B), depicting the accommodation of acyl chains into a fatty acid accommodating sites contained in SBD as well NBD. To this end, two fatty acid (FA) binding sites have been demonstrated for Hsp70, each saturating at a 1:1 FA/protein ratio [61]. The structures of these fatty acid binding sites in Hsp70 [62] are, however not known.

Together with our data on Br_2PCs (Fig. 4), the results with Br_8CL imply the following mechanism. Approximately 2–3 CL molecules bind to Hsp70 and induce a conformational change in Hsp70, involving opening of hydrophobic cavities, which can accommodate brominated acyl chains of PCs. Accordingly, the Br-containing *sn*-2 acyl chains would reverse their orientation extending out of the bilayer and becoming accommodated into hydrophobic crevices in Hsp70. Notably, this configuration results in a hydrophobic association of Hsp70 with the bilayers, yet without penetration of the protein into the bilayer hydrocarbon region [63]. Our data are in keeping with extended lipid acyl chains intercalating into SBD. Notably, this acyl chain intercalation could, in addition to involving acyl chain binding cavities [62], also reflect loosening of the tertiary structure of Hsp70 upon induction of the molten globule (MG) state by SBD, similar to α-lactalbumin [64], in keeping with the access of AcrA to the Trps. The far UV-CD spectra measured (Fig. 11, panel A) confirm the above structural change upon membrane binding. As demonstrated for cytochrome c [65–67] the above two mechanisms are not mutually exclusive [33]. It seems feasible that conformational changes induced by CL in the NBD of Hsp70, are further reflected in the conformations of the adjacent SBD, possibly promoting its transition into the MG, allowing the accommodation of brominated PC acyl chains into hydrophobic binding sites in SBD, similar to that described for α-lactalbumin [64].

Taken together the present results indicated SBD to adopt the MG conformation in the presence of CL and BMP. First, red shifts in Trp emission are seen in the presence of CL/PC LUV (Table 1). Second augmented quenching by AcrA is evident for W580 with CL/PC LUV, in keeping with more loose tertiary structure (Fig. 8, panel D). Third, our data are in keeping with extended lipid acyl chains intercalating into NBD and SBD.

The quenching of Trp by Br_4BMP in BMP/PC LUV is more efficient for W90 than for W580, confirming our previous observation that NBD contains a specific and pH-dependent binding site for BMP. The weak quenching by Br_2PCs in the presence of BMP (Fig. 12, panel A) could result from BMP occupying phospholipid binding sites in Hsp70 with extension of one of its acyl chains into hydrophobic cavities within Hsp70, similar to CL. In conclusion, Hsp70 NBD and SBD appear to bind peripherally onto the BMP/PC bilayer surface, analogously to a CL/PC membrane. Taking into account the resemblance of the structures of BMP and CL it is not surprising that the interactions of these lipids with Hsp70 are similar. BMP is highly enriched in the membranes of lysosomes and late endosomes [68]. The association and localization of Hsp70 to the lysosomal membranes leads to a cytoprotective effect and interferes with lysosomal cell death pathways [69,70]. Hsp70–

Table 2
Values for the Stern–Volmer quenching constants K_{sv} (M^{-1}) for 60 mM AcrA with 0.4 μM Hsp70 and the indicated constructs, in the presence of the indicated liposomes (95 μM total phospholipid, corresponding to L/P ≈ 234) and at pH 7.4 and 6.0.

		Hsp70	Hsp70-W90F (W580)	Hsp70-W580F (W90)	Hsp70-ΔNBD (SBD)	Hsp70-ΔSBD (NBD)
POPC	pH 7.4	1.85	2.52	1.34	4.16	0.13
	pH 6.0	1.88	1.69	1.11	3.67	0.43
CL/PC ($X_{CL} = 0.2$)	pH 7.4	3.75	4.26	3.79	4.72	2.21
	pH 6.0	4.62	3.43	3.67	3.51	3.23
PS/PC ($X_{PS} = 0.2$)	pH 7.4	2.90	1.78	2.3	3.64	0.79
	pH 6.0	2.31	1.24	1.37	2.78	1.11

BMP interaction plays a crucial role in the activation of the acidic sphingomyelinase (aSM) and the subsequent stabilization of lysosomes by ceramide [30]. Direct interaction between Hsp70 and BMP is required for this activation and downstream cytoprotective properties of Hsp70, and can be blocked by an antibody against a BMP [30]. Exact molecular mechanisms of activation of the aSM by Hsp70 are unclear. Similar to the mechanism proposed for phospholipase A2 [PLA2, 71] Hsp70 could sustain the lifetime of the catalytically active enzyme oligomers [72]. The above activation of Hsp70 can be readily assumed to require proper orientation of Hsp70 on the lipid bilayer surfaces. The extended phospholipid anchorage *via* BMP would provide a simple mechanism (Fig. 15, panel C).

Interactions between Hsp70 and PS differ from those with BMP and CL, with similar effects by PS/PC LUV on the two domains. Hsp70 has been shown to be enriched on the outer surface of the plasma membrane of cancer cells [73]. While ganglioside Gb3 could contribute to the binding of Hsp70 to the cancer cell surface [74], it is of interest that there is a loss of the asymmetric distribution of PS in the plasma membrane of cancer cells, with exposure of this lipid in the outer surface of cancer cells and vascular endothelial cell of cancerous tissues [75]. This expression of PS in cancer cell outer surface has been suggested to provide molecular targets for cancer cell abrogating amyloid forming host defense peptides [HDP, 35,55,76].

Recent advances in our understanding of the molecular level mechanisms underlying protein folding/aggregation disorders emphasize the role of membrane lipids in triggering protein aggregation and oligomerization into cytotoxic intermediates [76,77]. These advances underlie the importance of understanding of the molecular level mechanisms responsible for the membrane attachment of Hsp70. Both Hsp70 and Hsc70 bind to phosphatidylserine [78] and induce liposome aggregation [31], form ATP/ADP sensitive cation channels [25] and also larger pores [24]. Aggregation and oligomerization of Hsp70 in the presence of PS causes the formation of membrane bound oligomers, arranged into pores and as well as larger membrane permeabilizing structures, characteristically to an array of amyloid type fibrils [25]. The presence of PS in the outer surface of the plasma membrane has been suggested to be diagnostic for tumors [79–82], and could explain the presence of Hsp70 in the plasma membrane of cancer cells but not in normal cells with comparable cytosolic levels of Hsp70 [21], thus potentially conveying resistance of these cells to HDP that also bind PS [55,76], protecting cancer cells from apoptosis/necrosis induced by HDP.

In contrast to PS, CL does not appear to compete with Br_2PCs for protein binding. The above findings for PS/PC LUV could be explained by the following mechanism. Accordingly, PS could attach Hsp70 to the bilayer surface (Fig. 15, panel D) by adopting the extended conformation [57]. Additionally, the lack of quenching by Br_2PC in the presence of PS (Figs. 4 and 6, panels E & F) is likely to result from POPS occupying phospholipid binding sites in Hsp70 with extension of the PS *sn*-2 acyl chains into hydrophobic cavities within Hsp70. The reason may be electrostatically driven preferred interactions between the anionic PS head group and cationic residues in Hsp70.

Our findings suggest that the organelle specific distribution of Hsp70 is determined by specific Hsp70–phospholipid interactions with BMP, CL, and PS, localizing this chaperone in lysosomes, mitochondria, and on the outer surface of cancer cells, respectively. Along these lines we could also demonstrate Hsp70 to bind to POPC LUV containing N-acylphosphatidylethanolamine ($X = 0.2$, Fig. S6, [83]). It seems feasible to assume that further lipid ligands for Hsp70 may remain to be discovered, the formation of which in organelles potentially causing redistribution of Hsp70 within cells.

The possible functional significance of the present results is perhaps best understood within the framework of the current views on protein aggregation and misfolding leading to cytotoxic, lytic intermediates and amyloid formation [55,76,84–86] and reversal of this process by Hsp70. Recent studies have revealed apoptosis to be triggered by partially unfolded polypeptides aggregating into toxic oligomers on membrane surfaces and causing the permeabilization of lipid bilayers in cellular membranes [76]. Several lines of evidence obtained from a number of laboratories and dealing with different cytotoxic peptides have merged to suggest a common underlying mechanism, in which membranes containing either negatively charged and/or oxidized phospholipid species cause the accumulation of the cytotoxic peptides onto the membrane surface and induce their aggregation and subsequent conversion to amyloid-like aggregates, with intermediate cytotoxic oligomers being responsible for killing the targeted cells and causing loss of tissue function in conditions such as Alzheimer's and Parkinson's disease, Huntington disease, prion disease, age related macular degeneration, and type 2 diabetes [55,76,87]. Importantly, the same underlying mechanisms involving lipids has been recently concluded to be responsible for the targeting and cell death induced by host defense peptides [55,88], the latter thus providing an example of a novel type of functional amyloid. In keeping with amyloid formation by HDP as well as by endostatin [35], Congo red staining deposits have been observed in tumors irrespective of their anatomic location [89,90]. Hsp70 has been shown to counteract amyloid formation *in vitro* by Alzheimer Aβ peptide [85] and α-synuclein in a Parkinson disease model [91]. In addition to counteracting the aggregation and fibril formation by amylin [92], Aβ-peptide [85], and α-synuclein *in vitro* [93] Hsp70 also suppresses neurodegeneration in several animal models of protein aggregation and folding diseases [94–97]. In Huntington disease (HD) Hsp70 localizes in the inclusion bodies formed by the mutant huntingtin [87]. Hsp70 may also reduce the toxic impact of amyloid forming HDP [55,88] in cancer cells. Accordingly, the overexpression of Hsp70 in malignant tumors and its localization on the outer surface of cancer cells suggest that an efficient elimination of cytotoxic HDP aggregates by Hsp70 could be responsible for the promotion of cancer by this chaperone, in keeping with the poor prognosis and malignancy of highly Hsp70 expressing tumors [98]. The above mechanism would also comply with the apparent protective effect from cancer by neurodegenerative disorders, and *vice versa*, in addition to the role of oxidized lipids in promoting aggregation of cytotoxic peptides [99]. The above correlation emphasize the importance of understanding the structural characteristics and membrane association of Hsp70, relating to its chaperone function reversing the unfolding and formation of cytotoxic protein oligomers on cell membranes [100].

We recently showed Hsp70 to activate aSM in cultured cells [30]. We have suggested a novel type of functional amyloid formation in control of the activity of PLA2, with low activity enzyme monomers converting into highly active oligomers and subsequently to inactive amyloid, this process acting as a thermodynamic on–off switch for PLA2 activity [72], upon processing of the enzyme in the protein folding/aggregation free energy landscape. Along these lines we also showed Hsp70 to activate PLA2 *in vitro* in ATP-dependent manner and suggested this activation to result from Hsp70 prolonging the lifetime of the high activity oligomers, counteracting its inhibition by conversion into amyloid-like aggregates [71].

From a mechanistic point of view, with the formation and action of toxic peptide oligomers in lipid membrane surfaces, the localization of Hsp70 on these surfaces would allow its interactions with the aggregating substrate proteins, with electrostatic interactions and extended phospholipid anchorage between the membrane and Hsp70 retaining and orienting this enzyme strictly on the lipid membrane interface, and allowing the binding of the substrate proteins to SBD. Adoption of the molten globule conformation by SBD could be of functional significance allowing SBD to become transiently immersed into a lipid bilayer, in keeping with the observed transfer of the subunit CCT1, the substrate binding apical domain of the CCT/TRiC chaperone through cellular membranes [97]. Although the latter studies were conducted with a construct containing His-tag, the hydrophobic surface exposure of molten globule state complies with its partitioning with bilayer interior. For SBD this would mean that it would be able to attach also to substrate sequences [48] which localize within the hydrophobic region of the lipid bilayer.

Acknowledgements

This study was supported by the European Science Foundation EuroMEMBRANE CRP OXPL, Finnish Academy, the Sigrid Jusélius Foundation (PKJK), Association for International Cancer Research and Danish Medical Research Council (MJ). The authors wish to thank Prof. Galyna Gorbenko for helpful discussions.

Appendix A. Supplementary data

Sequence for the Hsp70 and shifts in the spectral center of mass ($\Delta\lambda$) of Trp fluorescence. Relative fluorescence intensities, and Trp quenching by AcrA and brominated lipids of Hsp70, Hsp70-ΔNBD (SBD), and Hsp70-ΔSBD. Supplementary data to this article can be found online at http://dx.doi.org/10.1016/j.bbamem.2014.01.022.

References

[1] F.U. Hartl, J. Martin, Molecular chaperones in cellular protein folding, Curr. Opin. Struct. Biol. 5 (1995) 92–102.
[2] M. Daugaard, M. Rohde, M. Jäättelä, The heat shock protein 70 family: highly homologous proteins with overlapping and distinct functions, FEBS Lett. 581 (2007) 3702–3710.
[3] E.J. Levy, J. McCarty, B. Bukau, W.J. Chirico, Conserved ATPase and luciferase refolding activities between bacteria and yeast Hsp70 chaperones and modulators, FEBS Lett. 368 (1995) 435–440.
[4] S. Lindquist, E.A. Craig, The heat-shock proteins, Annu. Rev. Genet. 22 (1988) 631–677.
[5] M.M. Simon, A. Reikerstorfer, A. Schwarz, C. Krone, T.A. Luger, M. Jäättelä, T. Schwarz, Heat shock protein 70 overexpression affects the response to ultraviolet light in murine fibroblasts. Evidence for increased cell viability and suppression of cytokine release, J. Clin. Invest. 95 (1995) 926–933.
[6] B.C. Freeman, M.P. Myers, R. Schumacher, R.I. Morimoto, Identification of a regulatory motif in Hsp70 that affects ATPase activity, substrate binding and interaction with HDJ-1, EMBO J. 14 (1995) 2281–2292.
[7] A. Buchberger, H. Theyssen, H. Schroder, J.S. McCarty, G. Virgallita, P. Milkereit, J. Reinstein, B. Bukau, Nucleotide-induced conformational changes in the ATPase and substrate binding domains of the DnaK chaperone provide evidence for interdomain communication, J. Biol. Chem. 270 (1995) 16903–16910.
[8] K.L. Fung, L. Hilgenberg, N.M. Wang, W.J. Chirico, Conformations of the nucleotide and polypeptide binding domains of a cytosolic Hsp70 molecular chaperone are coupled, J. Biol. Chem. 271 (1996) 21559–21565.
[9] C.K. Kassenbrock, R.B. Kelly, Interaction of heavy chain binding protein (BiP/GRP78) with adenine nucleotides, EMBO J. 8 (1989) 1461–1467.
[10] T.K. Nemoto, Y. Fukuma, H. Itoh, T. Takagi, T. Ono, A disulfide bridge mediated by cysteine 574 is formed in the dimer of the 70-kDa heat shock protein, J. Biochem. 139 (2006) 677–687.
[11] C.E. Angelidis, I. Lazaridis, G.N. Pagoulatos, Aggregation of hsp70 and hsc70 in vivo is distinct and temperature-dependent and their chaperone function is directly related to non-aggregated forms, Eur. J. Biochem. 259 (1999) 505–512.
[12] J. Nylandsted, K. Brand, M. Jäättelä, Heat shock protein 70 is required for the survival of cancer cells, Ann. N. Y. Acad. Sci. 926 (2000) 122–125.
[13] J. Nylandsted, W. Wick, U.A. Hirt, K. Brand, M. Rohde, M. Leist, M. Weller, M. Jäättelä, Eradication of glioblastoma, and breast and colon carcinoma xenografts by Hsp70 depletion, Cancer Res. 62 (2002) 7139–7142.
[14] M. Jäättelä, Escaping cell death: survival proteins in cancer, Exp. Cell Res. 248 (1999) 30–43.
[15] M. Jäättelä, Over-expression of hsp70 confers tumorigenicity to mouse fibrosarcoma cells, Int. J. Cancer 60 (1995) 689–693.
[16] D.R. Ciocca, G.M. Clark, A.K. Tandon, S.A. Fuqua, W.J. Welch, W.L. McGuire, Heat shock protein hsp70 in patients with axillary lymph node-negative breast cancer: prognostic implications, J. Natl. Cancer Inst. 85 (1993) 570–574.
[17] K. Nanbu, I. Konishi, M. Mandai, H. Kuroda, A.A. Hamid, T. Komatsu, T. Mori, Prognostic significance of heat shock proteins HSP70 and HSP90 in endometrial carcinomas, Cancer Detect. Prev. 22 (1998) 549–555.
[18] B. Farkas, M. Hantschel, M. Magyarlaki, B. Becker, K. Scherer, M. Landthaler, K. Pfister, M. Gehrmann, C. Gross, A. Mackensen, G. Multhoff, Heat shock protein 70 membrane expression and melanoma-associated marker phenotype in primary and metastatic melanoma, Melanoma Res. 13 (2003) 147–152.
[19] G. Multhoff, C. Botzler, L. Jennen, J. Schmidt, J. Ellwart, R. Issels, Heat shock protein 72 on tumor cells: a recognition structure for natural killer cells, J. Immunol. 158 (1997) 4341–4350.
[20] J. Nylandsted, M. Gyrd-Hansen, A. Danielewicz, N. Fehrenbacher, U. Lademann, M. Hoyer-Hansen, E. Weber, G. Multhoff, M. Rohde, M. Jäättelä, Heat shock protein 70 promotes cell survival by inhibiting lysosomal membrane permeabilization, J. Exp. Med. 200 (2004) 425–435.
[21] G. Multhoff, C. Botzler, M. Wiesnet, E. Muller, T. Meier, W. Wilmanns, R.D. Issels, A stress-inducible 72-kDa heat-shock protein (HSP72) is expressed on the surface of human tumor cells, but not on normal cells, Int. J. Cancer 61 (1995) 272–279.
[22] M. Hantschel, K. Pfister, A. Jordan, R. Scholz, R. Andreesen, G. Schmitz, H. Schmetzer, W. Hiddemann, G. Multhoff, Hsp70 plasma membrane expression on primary tumor biopsy material and bone marrow of leukemic patients, Cell Stress Chaperones 5 (2000) 438–442.
[23] C. Gross, W. Koelch, A. DeMaio, N. Arispe, G. Multhoff, Cell surface-bound heat shock protein 70 (Hsp70) mediates perforin-independent apoptosis by specific binding and uptake of granzyme B, J. Biol. Chem. 278 (2003) 41173–41181.
[24] G.M. Alder, B.M. Austen, C.L. Bashford, A. Mehlert, C.A. Pasternak, Heat shock proteins induce pores in membranes, Biosci. Rep. 10 (1990) 509–518.
[25] N. Arispe, A. De Maio, ATP and ADP modulate a cation channel formed by Hsc70 in acidic phospholipid membranes, J. Biol. Chem. 275 (2000) 30839–30843.
[26] D. Mamelak, C. Lingwood, Expression and sulfogalactolipid binding specificity of the recombinant testis-specific cognate heat shock protein 70, Glycoconj. J. 14 (1997) 715–722.
[27] D. Mamelak, C. Lingwood, The ATPase domain of hsp70 possesses a unique binding specificity for 3′-sulfogalactolipids, J. Biol. Chem. 276 (2001) 449–456.
[28] I. Kurucz, B. Tombor, J. Prechl, F. Erdo, E. Hegedus, Z. Nagy, M. Vitai, L. Koranyi, L. Laszlo, Ultrastructural localization of Hsp-72 examined with a new polyclonal antibody raised against the truncated variable domain of the heat shock protein, Cell Stress Chaperones 4 (1999) 139–152.
[29] A.H. Broquet, G. Thomas, J. Masliah, G. Trugnan, M. Bachelet, Expression of the molecular chaperone Hsp70 in detergent-resistant microdomains correlates with its membrane delivery and release, J. Biol. Chem. 278 (2003) 21601–21606.
[30] T. Kirkegaard, A.G. Roth, N.H. Petersen, A.K. Mahalka, O.D. Olsen, I. Moilanen, A. Zylicz, J. Knudsen, K. Sandhoff, C. Arenz, P.K.J. Kinnunen, J. Nylandsted, M. Jäättelä, Hsp70 stabilizes lysosomes and reverts Niemann–Pick disease-associated lysosomal pathology, Nature 463 (2010) 549–553.
[31] N. Arispe, M. Doh, A. De Maio, Lipid interaction differentiates the constitutive and stress-induced heat shock proteins Hsc70 and Hsp70, Cell Stress Chaperones 7 (2002) 330–338.
[32] H.J. Woo, J. Jiang, E.M. Lafer, R. Sousa, ATP-induced conformational changes in Hsp70: molecular dynamics and experimental validation of an in silico predicted conformation, Biochemistry 48 (2009) 11470–11477.
[33] E.K. Tuominen, C.J. Wallace, P.K.J. Kinnunen, Phospholipid-cytochrome c interaction: evidence for the extended lipid anchorage, J. Biol. Chem. 277 (2002) 8822–8826.
[34] M. Rytömaa, P.K.J. Kinnunen, Reversibility of the binding of cytochrome c to liposomes. Implications for lipid–protein interactions, J. Biol. Chem. 270 (1995) 3197–3202.
[35] H. Zhao, A. Jutila, T. Nurminen, S.A. Wickstrom, J. Keski-Oja, P.K.J. Kinnunen, Binding of endostatin to phosphatidylserine-containing membranes and formation of amyloid-like fibers, Biochemistry 44 (2005) 2857–2863.
[36] R.C. MacDonald, R.I. MacDonald, B.P. Menco, K. Takeshita, N.K. Subbarao, L.R. Hu, Small-volume extrusion apparatus for preparation of large, unilamellar vesicles, Biochim. Biophys. Acta 1061 (1991) 297–303.
[37] K. Emoto, J.M. Harris, J.M. Van Alstine, Grafting poly(ethylene glycol) epoxide to amino-derivatized quartz: effect of temperature and ph on grafting density, Anal. Chem. 68 (1996) 3751–3757.
[38] T.J. McIntosh, P.W. Holloway, Determination of the depth of bromine atoms in bilayers formed from bromolipid probes, Biochemistry 26 (1987) 1783–1788.
[39] J.M. East, A.G. Lee, Lipid selectivity of the calcium and magnesium ion dependent adenosinetriphosphatase, studied with fluorescence quenching by a brominated phospholipid, Biochemistry 21 (1982) 4144–4151.
[40] A. Chattopadhyay, E. London, Parallax method for direct measurement of membrane penetration depth utilizing fluorescence quenching by spin-labeled phospholipids, Biochemistry 26 (1987) 39–45.
[41] D.H. Tallmadge, J.S. Huebner, R.F. Borkman, Acrylamide quenching of tryptophan photochemistry and photophysics, Photochem. Photobiol. 49 (1989) 381–386.
[42] R. Sood, Y. Domanov, M. Pietiainen, V.P. Kontinen, P.K.J. Kinnunen, Binding of LL-37 to model biomembranes: insight into target vs host cell recognition, Biochim. Biophys. Acta 1778 (2008) 983–996.
[43] M.A. Andrade, P. Chacon, J.J. Merelo, F. Moran, Evaluation of secondary structure of proteins from UV circular dichroism spectra using an unsupervised learning neural network, Protein Eng. 6 (1993) 383–390.
[44] K. Zhu, A. Jutila, P.K.J. Kinnunen, Steady state and time resolved effects of guanidine hydrochloride on the structure of Humicola lanuginosa lipase revealed by fluorescence spectroscopy, Protein Sci. 9 (2000) 598–609.
[45] J.R. Lakowicz, Principles of Fluorescence Spectroscopy, Plenum, New York, 1983.
[46] S.H. White, G. von Heijne, How translocons select transmembrane helices, Annu. Rev. Biophys. 37 (2008) 23–42.
[47] R.A. Demel, W.S. Geurts van Kessel, R.F. Zwaal, B. Roelofsen, L.L. van Deenen, Relation between various phospholipase actions on human red cell membranes and the interfacial phospholipid pressure in monolayers, Biochim. Biophys. Acta 406 (1975) 97–107.
[48] W.F. Burkholder, X. Zhao, X. Zhu, W.A. Hendrickson, A. Gragerov, M.E. Gottesman, Mutations in the C-terminal fragment of DnaK affecting peptide binding, Proc. Natl. Acad. Sci. U. S. A. 93 (1996) 10632–10637.
[49] R. Loewenthal, J. Sancho, A.R. Fersht, Fluorescence spectrum of barnase: contributions of three tryptophan residues and a histidine-related pH dependence, Biochemistry 30 (1991) 6775–6779.
[50] C. Garrido, M. Brunet, C. Didelot, Y. Zermati, E. Schmitt, G. Kroemer, Heat shock proteins 27 and 70: anti-apoptotic proteins with tumorigenic properties, Cell Cycle 5 (2006) 2592–2601.
[51] Q. Liu, P. D'Silva, W. Walter, J. Marszalek, E.A. Craig, Regulated cycling of mitochondrial Hsp70 at the protein import channel, Science 300 (2003) 139–141.
[52] W. Neupert, M. Brunner, The protein import motor of mitochondria, Nat. Rev. Mol. Cell Biol. 3 (2002) 555–565.

[53] B.S. Polla, S. Kantengwa, D. Francois, S. Salvioli, C. Franceschi, C. Marsac, A. Cossarizza, Mitochondria are selective targets for the protective effects of heat shock against oxidative injury, Proc. Natl. Acad. Sci. U. S. A. 93 (1996) 6458–6463.
[54] V.A. Parsegian, Long-range physical forces in the biological milieu, Annu. Rev. Biophys. Bioeng. 2 (1973) 221–255.
[55] P.K.J. Kinnunen, Amyloid formation on lipid membrane surfaces, Open Biol. J. 2 (2009) 163–175.
[56] M. Rytömaa, P. Mustonen, P.K.J. Kinnunen, Reversible, nonionic, and pH-dependent association of cytochrome c with cardiolipin-phosphatidylcholine liposomes, J. Biol. Chem. 267 (1992) 22243–22248.
[57] P.K.J. Kinnunen, Fusion of lipid bilayers: a model involving mechanistic connection to HII phase forming lipids, Chem. Phys. Lipids 63 (1992) 251–258.
[58] P.K.J. Kinnunen, On the molecular-level mechanisms of peripheral protein–membrane interactions induced by lipids forming inverted non-lamellar phases, Chem. Phys. Lipids 81 (1996) 151–166.
[59] Y.G. Kim, E.J. Sohn, J. Seo, K.J. Lee, H.S. Lee, I. Hwang, M. Whiteway, M. Sacher, B.H. Oh, Crystal structure of bet3 reveals a novel mechanism for Golgi localization of tethering factor TRAPP, Nat. Struct. Mol. Biol. 12 (2005) 38–45.
[60] C. Meier, A.R. Aricescu, R. Assenberg, R.T. Aplin, R.J. Gilbert, J.M. Grimes, D.I. Stuart, The crystal structure of ORF-9b, a lipid binding protein from the SARS coronavirus, Structure 14 (2006) 1157–1165.
[61] P.T. Guidon Jr., L.E. Hightower, The 73 kilodalton heat shock cognate protein purified from rat brain contains nonesterified palmitic and stearic acids, J. Cell. Physiol. 128 (1986) 239–245.
[62] P.T. Guidon Jr., L.E. Hightower, Purification and initial characterization of the 71-kilodalton rat heat-shock protein and its cognate as fatty acid binding proteins, Biochemistry 25 (1986) 3231–3239.
[63] P.K.J. Kinnunen, A. Koiv, J.Y. Lehtonen, M. Rytomaa, P. Mustonen, Lipid dynamics and peripheral interactions of proteins with membrane surfaces, Chem. Phys. Lipids 73 (1994) 181–207.
[64] A.K. Lala, P. Kaul, P.B. Ratnam, Membrane–protein interaction and the molten globule state: interaction of alpha-lactalbumin with membranes, J. Protein Chem. 14 (1995) 601–609.
[65] A. Muga, H.H. Mantsch, W.K. Surewicz, Membrane binding induces destabilization of cytochrome c structure, Biochemistry 30 (1991) 7219–7224.
[66] G. Balakrishnan, Y. Hu, O.F. Oyerinde, J. Su, J.T. Groves, T.G. Spiro, A conformational switch to beta-sheet structure in cytochrome c leads to heme exposure. Implications for cardiolipin peroxidation and apoptosis, J. Am. Chem. Soc. 129 (2007) 504–505.
[67] V.E. Bychkova, A.E. Dujsekina, S.I. Klenin, E.I. Tiktopulo, V.N. Uversky, O.B. Ptitsyn, Molten globule-like state of cytochrome c under conditions simulating those near the membrane surface, Biochemistry 35 (1996) 6058–6063.
[68] T. Kolter, K. Sandhoff, Principles of lysosomal membrane digestion: stimulation of sphingolipid degradation by sphingolipid activator proteins and anionic lysosomal lipids, Annu. Rev. Cell Dev. Biol. 21 (2005) 81–103.
[69] U.P. Kodavanti, H.M. Mehendale, Cationic amphiphilic drugs and phospholipid storage disorder, Pharmacol. Rev. 42 (1990) 327–354.
[70] H. Schulze, T. Kolter, K. Sandhoff, Principles of lysosomal membrane degradation: cellular topology and biochemistry of lysosomal lipid degradation, Biochim. Biophys. Acta 1793 (2009) 674–683.
[71] A.K. Mahalka, C. Code, B. Rezaijahromi, T. Kirkegaard, M. Jäättelä, P.K.J. Kinnunen, Activation of phospholipase A2 by Hsp70 in vitro, Biochim. Biophys. Acta 1808 (2011) 2569–2572.
[72] C. Code, Y. Domanov, A. Jutila, P.K.J. Kinnunen, Amyloid-type fiber formation in control of enzyme action: interfacial activation of phospholipase A2, Biophys. J. 95 (2008) 215–224.
[73] G. Kroemer, M. Jäättelä, Lysosomes and autophagy in cell death control, Nat. Rev. Cancer 5 (2005) 886–897.
[74] M. Gehrmann, G. Liebisch, G. Schmitz, R. Anderson, C. Steinem, A. De Maio, G. Pockley, G. Multhoff, Tumor-specific Hsp70 plasma membrane localization is enabled by the glycosphingolipid Gb3, PLoS One 3 (2008) e1925.
[75] R.F. Zwaal, P. Comfurius, E.M. Bevers, Surface exposure of phosphatidylserine in pathological cells, Cell. Mol. Life Sci. 62 (2005) 971–988.
[76] P.K.J. Kinnunen, K. Kaarniranta, A.K. Mahalka, Protein-oxidized phospholipid interactions in cellular signaling for cell death: from biophysics to clinical correlations, Biochim. Biophys. Acta 1818 (2012) 2446–2455.
[77] G.P. Gorbenko, P.K.J. Kinnunen, The role of lipid–protein interactions in amyloid-type protein fibril formation, Chem. Phys. Lipids 141 (2006) 72–82.
[78] N. Arispe, M. Doh, O. Simakova, B. Kurganov, A. De Maio, Hsc70 and Hsp70 interact with phosphatidylserine on the surface of PC12 cells resulting in a decrease of viability, FASEB J. 18 (2004) 1636–1645.
[79] T. Utsugi, A.J. Schroit, J. Connor, C.D. Bucana, I.J. Fidler, Elevated expression of phosphatidylserine in the outer membrane leaflet of human tumor cells and recognition by activated human blood monocytes, Cancer Res. 51 (1991) 3062–3066.
[80] G. Multhoff, L.E. Hightower, Distinguishing integral and receptor-bound heat shock protein 70 (Hsp70) on the cell surface by Hsp70-specific antibodies, Cell Stress Chaperones 16 (2011) 251–255.
[81] K. Schutters, C. Reutelingsperger, Phosphatidylserine targeting for diagnosis and treatment of human diseases, Apoptosis 15 (2010) 1072–1082.
[82] H.P. Dong, A. Holth, L. Kleinberg, M.G. Ruud, M.B. Elstrand, C.G. Trope, B. Davidson, B. Risberg, Evaluation of cell surface expression of phosphatidylserine in ovarian carcinoma effusions using the annexin-V/7-AAD assay: clinical relevance and comparison with other apoptosis parameters, Am. J. Clin. Pathol. 132 (2009) 756–762.
[83] H.H. Schmid, P.C. Schmid, V. Natarajan, N-acylated glycerophospholipids and their derivatives, Prog. Lipid Res. 29 (1990) 1–43.
[84] C.M. Dobson, Protein folding and misfolding, Nature 426 (2003) 884–890.
[85] C.G. Evans, S. Wisen, J.E. Gestwicki, Heat shock proteins 70 and 90 inhibit early stages of amyloid beta-(1–42) aggregation in vitro, J. Biol. Chem. 281 (2006) 33182–33191.
[86] M. Bucciantini, E. Giannoni, F. Chiti, F. Baroni, L. Formigli, J. Zurdo, N. Taddei, G. Ramponi, C.M. Dobson, M. Stefani, Inherent toxicity of aggregates implies a common mechanism for protein misfolding diseases, Nature 416 (2002) 507–511.
[87] S.W. Davies, M. Turmaine, B.A. Cozens, M. DiFiglia, A.H. Sharp, C.A. Ross, E. Scherzinger, E.E. Wanker, L. Mangiarini, G.P. Bates, Formation of neuronal intranuclear inclusions underlies the neurological dysfunction in mice transgenic for the HD mutation, Cell 90 (1997) 537–548.
[88] A.K. Mahalka, P.K.J. Kinnunen, Binding of amphipathic alpha-helical antimicrobial peptides to lipid membranes: lessons from temporins B and L, Biochim. Biophys. Acta 1788 (2009) 1600–1609.
[89] B.E. Halliday, J.F. Silverman, J.L. Finley, Fine-needle aspiration cytology of amyloid associated with nonneoplastic and malignant lesions, Diagn. Cytopathol. 18 (1998) 270–275.
[90] S. Sahoo, W. Reeves, R.M. DeMay, Amyloid tumor: a clinical and cytomorphologic study, Diagn. Cytopathol. 28 (2003) 325–328.
[91] C. Huang, H. Cheng, S. Hao, H. Zhou, X. Zhang, J. Gao, Q.H. Sun, H. Hu, C.C. Wang, Heat shock protein 70 inhibits alpha-synuclein fibril formation via interactions with diverse intermediates, J. Mol. Biol. 364 (2006) 323–336.
[92] V. Chien, J.F. Aitken, S. Zhang, C.M. Buchanan, A. Hickey, T. Brittain, G.J. Cooper, K.M. Loomes, The chaperone proteins HSP70, HSP40/DnaJ and GRP78/BiP suppress misfolding and formation of beta-sheet-containing aggregates by human amylin: a potential role for defective chaperone biology in Type 2 diabetes, Biochem. J. 432 (2010) 113–121.
[93] M.M. Dedmon, J. Christodoulou, M.R. Wilson, C.M. Dobson, Heat shock protein 70 inhibits alpha-synuclein fibril formation via preferential binding to prefibrillar species, J. Biol. Chem. 280 (2005) 14733–14740.
[94] A. Sittler, R. Lurz, G. Lueder, J. Priller, H. Lehrach, M.K. Hayer-Hartl, F.U. Hartl, E.E. Wanker, Geldanamycin activates a heat shock response and inhibits huntingtin aggregation in a cell culture model of Huntington's disease, Hum. Mol. Genet. 10 (2001) 1307–1315.
[95] G.P. Lotz, J. Legleiter, R. Aron, E.J. Mitchell, S.Y. Huang, C. Ng, C. Glabe, L.M. Thompson, P.J. Muchowski, Hsp70 and Hsp40 functionally interact with soluble mutant huntingtin oligomers in a classic ATP-dependent reaction cycle, J. Biol. Chem. 285 (2010) 38183–38193.
[96] P.K. Auluck, H.Y. Chan, J.Q. Trojanowski, V.M. Lee, N.M. Bonini, Chaperone suppression of alpha-synuclein toxicity in a *Drosophila* model for Parkinson's disease, Science 295 (2002) 865–868.
[97] E.M. Sontag, L.A. Joachimiak, Z. Tan, A. Tomlinson, D.E. Housman, C.G. Glabe, S.G. Potkin, J. Frydman, L.M. Thompson, Exogenous delivery of chaperonin subunit fragment ApiCCT1 modulates mutant Huntingtin cellular phenotypes, Proc. Natl. Acad. Sci. U. S. A. 110 (2013) 3077–3082.
[98] M. Jäättelä, D. Wissing, P.A. Bauer, G.C. Li, Major heat shock protein hsp70 protects tumor cells from tumor necrosis factor cytotoxicity, EMBO J. 11 (1992) 3507–3512.
[99] P.K.J. Kinnunen, Cancer linked to Alzheimer disease but not vascular dementia, Neurology 75 (2010) 1215(Jaate).
[100] P.J. Muchowski, J.L. Wacker, Modulation of neurodegeneration by molecular chaperones, Nat. Rev. Neurosci. 6 (2005) 11–22.